

PREPARED FOR SUBMISSION TO JHEP

SEPTEMBER 3, 2025

Flat Space Holography via AdS/BCFT

Peng-Xiang Hao^a Naoki Ogawa^a Tadashi Takayanagi^{a,b} Takahiro Waki^a

^a*Center for Gravitational Physics and Quantum Information, Yukawa Institute for Theoretical Physics, Kyoto University, Kitashirakawa Oiwakecho, Sakyo-ku, Kyoto 606-8502, Japan*

^b*Inamori Research Institute for Science, 620 Suiginya-cho, Shimogyo-ku, Kyoto 600-8411, Japan*

E-mail: pxhao@yukawa.kyoto-u.ac.jp,
naoki.ogawa@yukawa.kyoto-u.ac.jp, takayana@yukawa.kyoto-u.ac.jp,
takahiro.waki@yukawa.kyoto-u.ac.jp

ABSTRACT: In this paper, we study a new class of AdS/BCFT setups, where the world-volumes of end-of-the-world branes (EOW branes) are given by flat spaces, to explore flat space holography from an AdS bulk. We show that they provide gravity duals of CFTs in the presence of null boundaries. Our holographic calculations lead to many new predictions on entanglement entropy, correlation functions and partition functions for CFTs with null boundaries. By considering a bulk region between two EOW branes, we present an AdS/BCFT explanation that the flat space gravity is dual to a Carrollian CFT (CCFT), including the swing surface calculation of entanglement entropy.

Contents

1	Introduction	2
2	AdS/BCFT Setups for Flat Space Holography	4
2.1	Flat EOW brane	5
2.2	Three setups of flat brane holography	7
2.3	Type I Setup	8
2.4	Type II Setup	8
2.5	Type III Setup	10
3	Holographic entanglement entropy	10
3.1	Holographic entanglement entropy in type I setup	11
3.2	Holographic entanglement entropy in type II setup	13
3.3	Holographic entanglement entropy in type III setup	17
4	Holographic correlation functions	20
4.1	Two-point Functions in type I Case	20
4.2	Two-point functions in type II Case	23
4.3	One-point functions in type I and II case	25
4.4	Type III Case	29
5	On-shell action in Euclidean Poincare AdS_3	32
5.1	Regularization by deforming the cut off surface	32
5.2	Regularization by deforming flat EOW branes to AdS ones	34
5.3	Comparison with boundary entropy	35
6	Euclidean Holography	35
6.1	Holographic Setup	35
6.2	On-shell action	36
7	Conclusions	38

A	BCFT with a null boundary	40
A.1	Free scalar model	40
A.2	Analytical continuation and conformal map	42
A.3	Moving mirror	43

1 Introduction

The idea of holography [1, 2] enables us to describe difficult problems in quantum gravity in terms of more tractable ones in dual quantum field theories. In particular, holography in anti de-Sitter space (AdS), i.e. the AdS/CFT [3–5], has been well-established. In the AdS/CFT, the gravity on $d + 1$ dimensional AdS becomes equivalent to a d dimensional conformal field theory (CFT), which lives on the boundary of the AdS. This duality was found by considering a setup where D-branes in string theory back-react to the geometry via the gravitational force, which leads to the AdS geometry. Moreover, the d dimensional conformal symmetry corresponds to the geometrical symmetry of $d + 1$ dimensional AdS.

On the contrary, holography in flat spacetime turns out to be more difficult to obtain in string theory, because flat spacetime does not need any source in string theory, as opposed to the AdS which was produced by D-branes. However, since the holography typically argues that a gravity on a certain spacetime is dual to a field theory on its boundary, we expect that a gravity in a Minkowski spacetime should be dual to its null boundary. In addition, the asymptotic symmetries that preserve the boundary structure, so-called BMS group, are useful to explore the holography [6, 7].

So far, there are two major approaches to holography in asymptotically flat spacetimes. The first one is the Flat/Carrollian CFT (CCFT) correspondence [8–10], where the dual field theory resides on the null boundary. The second one is the celestial holography [11–13], where dual CFTs live on the celestial sphere which is a codimension two. The relationship between these two ideas of holography has been understood better till now: [14–17]. In addition to these, which fully employ the symmetries, it would be desirable if we could have another argument which is a more top-down approach.

The purpose of this paper is to provide a new approach to the flat space holography. In particular, we would like to consider a method to embed it in the framework of AdS/CFT. This is because it allows us to understand the flat space holography as a

version of AdS/CFT, which is quite established and well understood. For this purpose, we employ the AdS/BCFT correspondence [18–20], which argues that the gravity dual of a CFT on a d dimensional manifold N_d with a conformal boundary (BCFT) is dual to a part of AdS geometry M_{d+1} which is surrounded by the manifold N_d and a surface Q_d called the end-of-the-world brane (EOW brane) such that $\partial M_{d+1} = N_d \cup Q_d$. One advantage of the AdS/BCFT is that we can extend the holographic calculation of entanglement entropy [21–23] to the setups with EOW branes by simply allowing the extremal surface can end on EOW branes [18, 19]. Another advantage is that it can have the third dual interpretation by regarding the CFT dual as a d dimensional CFT coupled to a d dimensional gravity on the EOW brane via the brane world holography [24–27].

The EOW branes, the most important ingredient of the AdS/BCFT, are characterized by values of tension T . Depending on values of tension, they are classified into three classes such that the induced metric on a given EOW brane becomes either AdS, dS or flat space. The most standard one is the AdS brane, which has successfully been applied to the black hole information problem [28, 29] as the holographic entanglement in the AdS/BCFT can explain the island formula [29, 30], which was explicitly confirmed in [31, 32]. For applications to cosmological models refer to [33–38]. The dS branes have not been completely well-understood because they are exotic from the viewpoint of CFTs as they are dual to space-like boundaries in CFTs [39–41]. Nevertheless, several interesting applications have been considered recently, including the gravity dual of cross cap states [42] and an embedding dS/CFT into AdS/BCFT [43].

The least studied EOW branes are the flat branes which are realized for special values of tension. Via the brane-world holography it is directly related to holography for flat spacetimes. Thus in the present paper we would like to explore properties of flat EOW branes in order to get insights on how the holography for flat spacetimes looks like. The AdS/BCFT approach allows us to compute various quantities such as entanglement entropy and correlation functions as we will show in this paper. Interestingly, flat EOW branes are dual to null boundaries in CFTs. Such boundaries in field theories have not been well-understood and are worth exploring by combining the field theoretic and holographic calculations.

Using a flat EOW brane, we will consider three setups, called type I, II and III (refer to Fig.3). In the type I and II model, the brane has a negative and positive tension, respectively. In the type I case, the CFT is defined on a diamond with null

boundaries, where the boundaries play a role similar to the final state projections. On the other hand, in the type II case, the CFT on the diamond is coupled to flat space gravity through the null boundaries. In the type II construction, we will find that our AdS/BCFT consideration reproduces the Flat/Carrollian CFT (CCFT) correspondence, where the Carrollian CFT is realized on the null boundary of the flat EOW brane. We can pick up purely the flat space gravity by sandwiching the bulk AdS region by two flat EOW branes and by applying the wedge holography [39], which is called the type III setup and can make the above argument clearer.

We will work out the holographic calculations of entanglement entropy and correlation functions, which are consistent with each other in the type I and II setup. In the type II case, we will see that the holographic entanglement includes an imaginary valued contribution, which can properly be regarded as the pseudo entropy [44] and is similar to the time-like entanglement entropy [45–47]. Thus this implies that the dual density matrix is not hermitian. In the type III setup, we will derive the swing surface prescription of holographic entanglement in flat space holography [48] from the AdS/BCFT. We will also discuss a Euclidean space version of flat space holography using the EOW brane, which implies that the gravity dual of a flat space is given by a point-like theory.

This paper is organized as follows. In section two, we present our three setups of AdS/BCFT with flat EOW branes. In section three, we present the calculation of holographic entanglement entropy in our AdS/BCFT with flat EOW branes. In section four, we compute one-point and two-point functions in our setups. In section five, we evaluate the on-shell action of our gravity duals. In section six, we analyze the Euclidean counterpart of our AdS/BCFT with flat EOW branes. In section seven, we summarize our conclusions and discuss future problems. In appendix A, we present a field theoretic analysis of the limit of light-like boundary in a two dimensional BCFT.

Note added: When we are finalizing this work, we noticed the independent preprint [49], which discusses flat EOW branes from different viewpoints.

2 AdS/BCFT Setups for Flat Space Holography

A d dimensional conformal field theory (CFT) defined on a manifold with boundaries with boundary conditions which preserve the boundary conformal symmetry $SO(2, d - 1)$ of the whole symmetry $SO(2, d)$ is called the boundary conformal field theory (BCFT). The gravity dual of d dimensional BCFT (BCFT $_d$) is given by a part

of AdS_{d+1} surrounded by the end-of-the-world brane (EOW brane), described by the surface Q . On this EOW brane, the following boundary condition is imposed so that the dual theory preserves the boundary conformal symmetry [18, 19]:

$$K_{ab} - Kh_{ab} = -Th_{ab}, \quad (2.1)$$

where K_{ab} and h_{ab} are extrinsic curvature and the induced metric of the EOW brane. The parameter T is called the tension of the EOW brane, which determines the profile of the brane. We have the following three classes of EOW branes depending on the values of the tension:

- (i) $|T| < \frac{d-1}{R}$: AdS brane in $\text{AdS}_{d+1} \leftrightarrow$ Time-like boundary in CFT_d
- (ii) $|T| = \frac{d-1}{R}$: Flat brane in $\text{AdS}_{d+1} \leftrightarrow$ Null boundary in CFT_d ,
- (iii) $|T| > \frac{d-1}{R}$: dS brane in $\text{AdS}_{d+1} \leftrightarrow$ Space-like boundary in CFT_d .

We can further generalize each EOW brane by introducing the matter fields on the brane as was done in the AdS brane [50, 51] and the dS brane [43], which breaks the boundary conformal invariance and thus can describe the boundary renormalization group flows. In particular, it would be intriguing to do this for our flat branes, though below we will be focusing on the case without any matter fields.

2.1 Flat EOW brane

The main purpose of this paper is to examine the second case (ii), which has not been well-studied in the context of holography till now. If we employ the brane-world holography idea to the AdS/BCFT, we can obtain the third interpretation in terms of the CFT on the d dimensional manifold coupled to a d dimensional gravity on the EOW brane along the boundaries, which is called the double holography and has been often employed to analyze the black hole information problems. If we apply this interpretation, we can regard the setup (ii) as a CFT coupled to a gravity on a flat spacetime. Therefore, we can embed the problem of the holography in flat spacetime, which is far from well-understood even now, into the AdS/BCFT setups, which is much more controllable.

Now let us present how the flat brane (ii) looks like explicitly. We consider both the Poincare and global AdS_{d+1} , whose metric looks like

$$\begin{aligned} ds^2 &= R^2 \left(\frac{dz^2 - dt^2 + \sum_{i=1}^{d-1} dx_i^2}{z^2} \right) \\ &= R^2 \left(-\cosh^2 \rho d\tau^2 + d\rho^2 + \sinh^2 \rho (d\phi^2 + \sin^2 \phi d\Omega^2) \right), \end{aligned} \quad (2.2)$$

respectively. $(\Omega_1, \Omega_2, \dots, \Omega_{d-1})$ describes the coordinate of a unit sphere S^{d-2} . These two coordinates are related explicitly via

$$\begin{aligned} X_0 &= R \cosh \rho \cos \tau = \frac{z}{2} \left(1 + \frac{R^2 + x^2 - t^2}{z^2} \right), \\ X_1 &= R \cosh \rho \sin \tau = \frac{Rt}{z}, \\ X_2 &= -R \sinh \rho \cos \phi = \frac{z}{2} \left(1 - \frac{R^2 - x^2 + t^2}{z^2} \right), \\ X_{i+2} &= R \sinh \rho \sin \phi \Omega_i = \frac{Rx_i}{z}, \quad (i = 1, 2, \dots, d-1). \end{aligned} \quad (2.3)$$

Note that the Poincare coordinate only covers a wedge of global AdS because

$$\frac{X_0 - X_2}{R} = \frac{R}{z} = \cosh \rho \cos \tau + \sinh \rho \cos \phi > 0, \quad (2.4)$$

as depicted in the left panel of Fig.1.

In the Poincare coordinate, the flat brane is very simply described such that z takes a constant value: $z = z_0$, whose induced metric is obviously flat. In terms of the global coordinate, this reads

$$\cosh \rho \cos \tau + \sinh \rho \cos \phi = \frac{R}{z_0}, \quad (2.5)$$

which is depicted in the left panel of Fig.2. This EOW brane intersects with the global AdS boundary $\rho = \rho_\infty \rightarrow \infty$ along the diamond:

$$\cos \tau + \cos \phi = 0, \quad (2.6)$$

which coincides with the boundary of Poincare AdS_3 as sketched in the right panel of Fig.1. At $\tau = 0$, it extends from the boundary point $(\rho, \phi) = (\infty, \pi)$ to the internal point $(\rho, \phi) = (\log \frac{R}{z_0}, 0)$ when $R > z_0$. When $R < z_0$, it extends to $(\rho, \phi) = (-\log \frac{R}{z_0}, \pi)$.

In the Euclidean global AdS, by setting $\tau = i\tau_E$, the EOW brane is described by

$$\cosh \rho \cosh \tau_E + \sinh \rho \cos \phi = \frac{R}{z_0}. \quad (2.7)$$

This is depicted in the right panel of Fig.2.

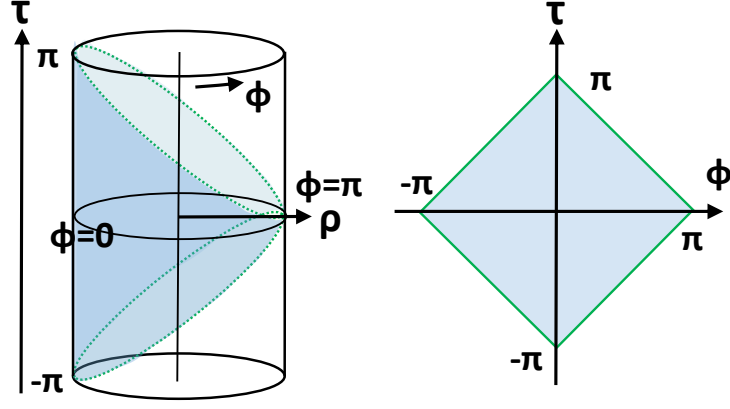


Figure 1. A sketch of Poincare AdS inside global AdS (left) and the boundary of Poincare AdS (right) in the coordinate of (τ, ϕ) .

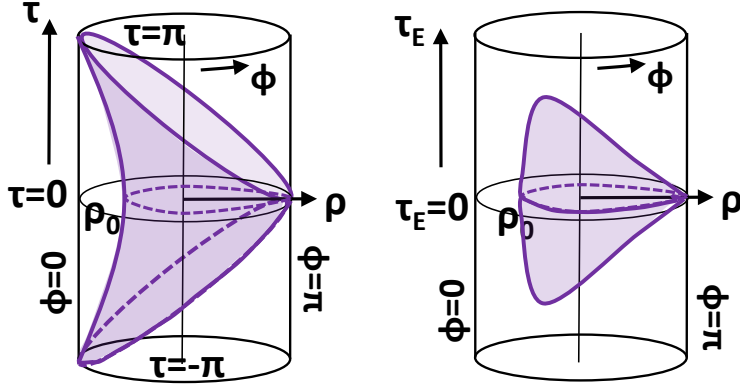


Figure 2. A sketch of the profile of a flat EOW brane in the Lorentzian global AdS (left) and in the Euclidean global AdS (right). We assume $R > z_0$.

2.2 Three setups of flat brane holography

Using this flat EOW brane (2.5), we would like to consider the following three different setups inside the global AdS called type I, type II and type III. They are defined by

$$\begin{aligned}
 \text{Type I} &: 0 < z < z_0, \\
 \text{Type II} &: z > z_0, \\
 \text{Type III} &: z_1 < z < z_2,
 \end{aligned} \tag{2.8}$$

which are sketched in Fig.3. Note that the gravity dual of type I includes the whole AdS boundary at $z = 0$, which ends on the flat EOW brane at $z = z_0$. The gravity dual of type II is the complement of that of type I. For the type III, we consider two EOW flat branes $z = z_1$ and $z = z_2$ and picks up the region between them. Below we will explain how the holography looks like.

2.3 Type I Setup

The gravity dual in the type I case is given by the region between the AdS boundary and the flat EOW brane as sketched in the top left panel of Fig.3. The AdS boundary is the diamond (times the celestial sphere S^{d-2}):

$$|\tau + \phi| \leq \pi, \quad |\tau - \phi| \leq \pi, \quad (2.9)$$

whose boundary is the solution to (2.6) as in the top middle panel of Fig.3. Thus, its CFT dual is given by a CFT defined on the diamond (2.9), with the null boundaries. The degrees of freedom of these null boundaries is expected to be equivalent to those of the flat EOW brane. From the observer in the gravity dual, this flat brane has the negative tension $T = -\frac{d-1}{R}$.

The Euclidean setup of type I is shown in the top right panel of the same figure. This covers the whole region of the AdS boundary and thus its CFT dual describes a point-like defect in a CFT on $R \times S^{d-1}$.

2.4 Type II Setup

Instead, in the type II setup, we pick up the interior region of the flat EOW brane with $T = \frac{d-1}{R}$, as depicted in the middle left panel of Fig.3. This region can be infinitely extended in both the future and past direction $\tau \rightarrow \pm\infty$, which creates the AdS boundary region in these directions. Therefore, its CFT dual looks like the CFT which surrounds the diamond (2.9) and its null boundaries. Via the double holography, this is equivalent to the CFT coupled to the flat space gravity on the diamond as depicted in the middle center panel of Fig.3. Hence, this provides an interesting model which includes the flat space holography.

The Euclidean setup of type II is shown in the middle right panel of the same figure. Its AdS boundary includes only the point $\phi = \pi$. Therefore, the gravity in the type II region is expected to dual to a point-like theory.

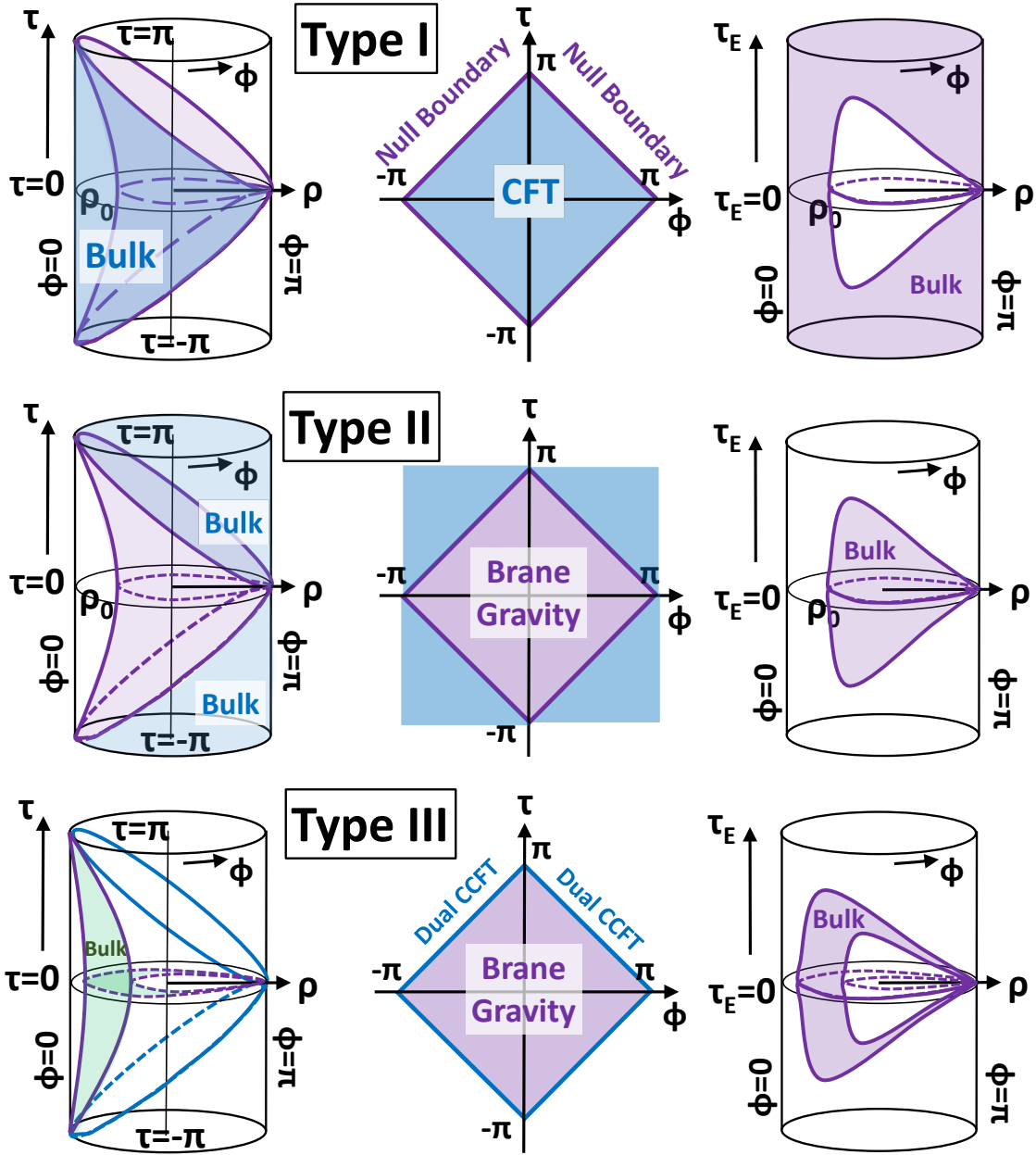


Figure 3. Sketches of the three setups: type I, II and III from the top to the bottom. The left panels show the regions of the gravity dual in the global AdS. The middle ones describe the dual two dimensional theories. The right ones show the Euclidean setups.

2.5 Type III Setup

In the type II setup, the field theory dual includes the large ‘bath’ theory, which extends outside of the diamond. To extract the flat space holography, we can remove the large bath by adding one more flat EOW brane and by focusing on the region between the two EOW branes, sketched in the bottom panels of Fig.3. This consideration leads to the type III setup. The AdS boundary of this model only consists of the null edges of the diamond. Thus, its CFT dual is given by a $d - 1$ -dimensional Carrollian CFT (CCFT $_{d-1}$) which lives on the null lines $|\tau + \phi| = |\tau - \phi| = \pi$. Note that the insertion of the flat EOW brane breaks the isometry of the AdS $_{d+1}$ with the remaining symmetry group $ISO(1, d - 1)$, which is also the global symmetry group of the CCFT $_{d-1}$. Via the double holography, we can also regard this as the flat space gravity on the diamond. Thus, this provides an interesting setup of flat space holography.

In the Euclidean setup of type III, there is also the region surrounded by the two EOW branes, and its AdS boundary only includes the point $\phi = \pi$, which shows that the gravity in the type III region should again be dual to a point-like theory.

3 Holographic entanglement entropy

In this section, we calculate the entanglement entropy of the subsystem in the dual field theory holographically in the AdS $_3$ in type I, II setups and in AdS $_4$ in type III setup by holographic entanglement entropy formula [21–23].

In the type I, II setups, given the presence of an EOW brane in the bulk AdS $_3$ spacetime, two types of extremal surfaces arise according to the AdS/BCFT correspondence. The first type is the connected extremal surface, denoted by $\Gamma_{\mathcal{A}}^{\text{con}}$, with its boundary located solely on the entangling surface $\partial\mathcal{A}$. The second type is the disconnected surface $\Gamma_{\mathcal{A}}^{\text{dis}}$, anchored on the EOW brane and also $\partial\mathcal{A}$. Specifically, $\Gamma_{\mathcal{A}}^{\text{dis}}$ represents geodesics that originate from one of the entangling surfaces and terminate on the EOW brane. The endpoint of $\Gamma_{\mathcal{A}}^{\text{dis}}$ on the EOW is determined by the extremization conditions. The contributions to the entanglement entropy are denoted as $S_{\mathcal{A}}^{\text{con}}$ and $S_{\mathcal{A}}^{\text{dis}}$ for the connected and disconnected surfaces, respectively. By applying the holographic entanglement entropy (HEE) formula, we can determine the entanglement entropy of the bath,

$$S_{\mathcal{A}} = \min\{S_{\mathcal{A}}^{\text{con}}, S_{\mathcal{A}}^{\text{dis}}\} = \min\left\{\frac{\text{Area}(\Gamma_{\mathcal{A}}^{\text{con}})}{4G_{\text{N}}}, \frac{\text{Area}(\Gamma_{\mathcal{A}}^{\text{dis}})}{4G_{\text{N}}}\right\}, \quad (3.1)$$

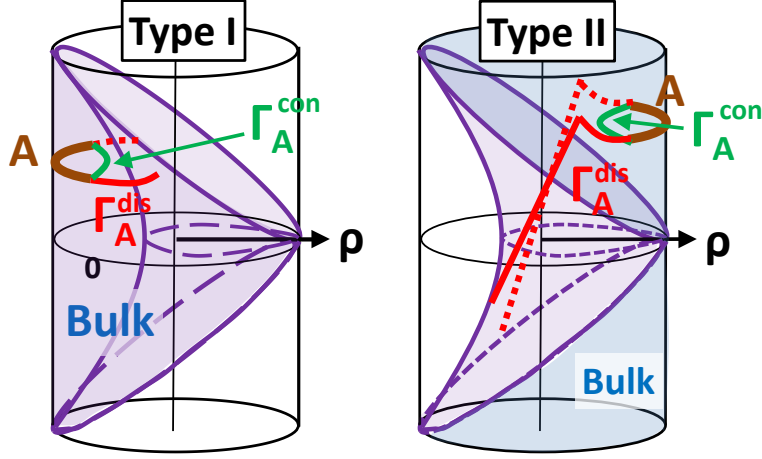


Figure 4. A sketch of calculations of holographic entanglement entropy in type I (left) and type II (right) setup for AdS_3 . The connected and disconnected geodesic are described by the green and red curves.

where G_N denotes the Newton's constant for the gravitational theory in the AdS_3 bulk spacetime. We set the AdS radius to be unit $R = 1$ and the central charge of the dual two-dimensional CFT is given by $c = \frac{3}{2G_N}$. In the AdS_3 case, the area of the extremal surface becomes the geodesic length which can be derived from the chordal distance,

$$\cosh D_{\text{AdS}} = -X(1) \cdot X(2), \quad (3.2)$$

where the AdS radius R is taken to be 1, $X(i)$ represents the coordinate of the i -th point in the embedding coordinate and the inner product is calculated by the metric of the embedding spacetime.

We examine both connected and disconnected extremal surfaces and determine their lengths in type I and type II configurations, as detailed in subsections (3.1) and (3.2), and illustrated in Fig. 4.

3.1 Holographic entanglement entropy in type I setup

It is convenient to consider the type I setup in the Poincare AdS coordinate,

$$ds^2 = \frac{1}{z^2}(-dt^2 + dz^2 + dx^2), \quad (3.3)$$

so that the length is

$$\cosh D_{\text{Poin}} = \frac{x_{12}^2 - t_{12}^2 + z_1^2 + z_2^2}{2z_1 z_2}, \quad (3.4)$$

for the geodesic connecting two points (z_1, t_1, x_1) and (z_2, t_2, x_2) in AdS_3 , which can be derived from (3.2) and the embedding (2.3) for the Poincare coordinate, where $x_{ij} = x_i - x_j$, $t_{ij} = t_i - t_j$. The interval \mathcal{A} is labeled by its two endpoints on the asymptotic boundary of the AdS on $z = 0$,

$$\partial\mathcal{A} = \{A_1 = (z = 0, t_1, x_1), A_2 = (z = 0, t_2, x_2)\}. \quad (3.5)$$

Connected phase contribution The holographic entanglement entropy from the connected phase is given by the length of the geodesic connecting the two endpoints with proper regulator on $z = z_c \rightarrow 0$,

$$S_I^{\text{con}} = \frac{D_{12}}{4G_N} = \frac{1}{4G_N} (\log(x_{12}^2 - t_{12}^2) - \log z_{c1} - \log z_{c2}). \quad (3.6)$$

In the original global coordinate, this is written as

$$S_I^{\text{con}} = \frac{D_{12}}{4G_N} = \frac{1}{4G_N} \left(\log \frac{\cos \tau_{12} - \cos \phi_{12}}{2} - 2 \log \epsilon \right), \quad (3.7)$$

which is the same as the entanglement entropy for the interval on the cylinder in CFT_2 . Here we write the UV cut off in the global coordinate $\epsilon = e^{-\rho_\infty}$ in terms of those in the Poincare AdS z_{c1} and z_{c2} via $z_{c1} = \frac{2}{\cos \tau_1 + \cos \phi_1} \epsilon$ and similar for z_{c2} as follows from (2.3).

Disconnected phase contribution To get the contribution from the disconnected phase, we should consider the geodesic connecting one of the endpoints of the interval, e.g., A_1 without loss of generality, and the point $A_3(z_0, t_3, x_3)$ on the EOW brane $z = z_0$, whose length is given by

$$D_{13} = \log \left(\frac{x_{13}^2 - t_{13}^2 + z_0^2}{z_0} \right) - \log z_{c1}, \quad (3.8)$$

where we have considered the regulator on $z_{c1} \rightarrow 0$. The holographic entanglement entropy from the disconnected phase is determined by the extremal condition

$$S_{\mathcal{A}}^{\text{dis}} = \text{Ext}_{A_3} \frac{\text{Area}(D_{13})}{4G_N} + \text{Ext}_{A_4} \frac{\text{Area}(D_{24})}{4G_N}, \quad (3.9)$$

where the counter-partner of the geodesic connecting the endpoint A_2 and the point A_4 on the brane is also taken into consideration. This, in turn, gives the location of A_3 ,

$$\partial_{t_3} D_{13} = 0, \quad \partial_{x_3} D_{13} = 0. \quad (3.10)$$

It yields the solution as

$$t_3 = t_1, \quad x_3 = x_1. \quad (3.11)$$

A further calculation of the second derivatives of the geodesic length shows that

$$\partial_{t_3}^2 D_{13} < 0, \quad \partial_{x_3}^2 D_{13} > 0, \quad (3.12)$$

which shows the disconnected extremal surface extremized along the flat brane is locally maximal with respect to temporal variations and minimal with respect to spatial variations. Consequently, it is a proper candidate surface for the holographic entanglement entropy, as it is reasonable to infer that this type of extremal surface corresponds to the dominant saddle in the Euclidean path integral for calculating entanglement entropy.

With the solution (3.11), we find the contribution to the holographic entanglement entropy from the length of the geodesic in disconnected phase

$$S_I^{\text{dis}} = 2 \frac{D_{\text{dis}}}{4G_N} = 2 \log \frac{z_0}{z_{c1}}, \quad (3.13)$$

where we have considered the contribution from the other geodesic connecting A_2 and the point on the flat EOW brane, resulting in an additional identical contribution.

Thus we can determine the disconnected holographic entanglement entropy in the (τ, ϕ) coordinate system as follows

$$S_{I,\text{cyl}}^{\text{dis}} = \frac{D_{\text{dis},13}}{4G_N} + \frac{D_{\text{dis},24}}{4G_N} = \frac{1}{4G_N} \left(\log \frac{z_0(\cos \tau_1 + \cos \phi_1)}{2\epsilon} + \log \frac{z_0(\cos \tau_2 + \cos \phi_2)}{2\epsilon} \right), \quad (3.14)$$

where $\epsilon = e^{-\rho_\infty}$ is the UV cut off in the global AdS_3 , which is related to z_c via $z_c = \frac{2}{\cos \tau_{1,2} + \cos \phi_{1,2}} \epsilon$ as (2.3). The actual holographic entanglement entropy is given by the minimum among the connected entropy (3.7) and disconnected one (3.14), by applying the general rule (3.1).

3.2 Holographic entanglement entropy in type II setup

Compared to the type I setup, the situation is significantly altered in the type II setup, where the dual field theory with large bath extends out of the Poincare patch. We then consider the global AdS_3 coordinate,

$$ds^2 = -\cosh^2 \rho d\tau^2 + d\rho^2 + \sinh^2 \rho d\phi^2. \quad (3.15)$$

The corresponding field theory covers the region

$$\cos \phi + \cos \tau < 0, \quad (3.16)$$

in the asymptotic boundary $\rho \rightarrow \infty$ of the AdS_3 spacetime. The flat EOW brane is described by (2.5). In this global coordinate, the geodesic length is represented by

$$\cosh D_{\text{global}} = \cos(\tau_1 - \tau_2) \cosh \rho_1 \cosh \rho_2 - \cos(\phi_1 - \phi_2) \sinh \rho_1 \sinh \rho_2, \quad (3.17)$$

for the geodesic connecting two points (ρ_1, τ_1, ϕ_1) and (ρ_2, τ_2, ϕ_2) . We specify the interval \mathcal{A} by the two endpoints,

$$\partial \mathcal{A} = \{A_1 = (\rho = \rho_\infty \rightarrow \infty, \tau_1, \phi_1), A_2 = (\rho = \rho_\infty \rightarrow \infty, \tau_2, \phi_2)\}. \quad (3.18)$$

Connected phase contribution The holographic entanglement entropy from the connected phase is given by the length of the geodesic connecting the two endpoints A_1, A_2 and then expand with respect to the regulator $\rho_\infty = -\log \epsilon$ at $\epsilon = 0$,

$$S_{II}^{\text{con}} = \frac{D_{12}}{4G_N} = \frac{1}{4G_N} \left(\log \frac{\cos \tau_{12} - \cos \phi_{12}}{2} - 2 \log \epsilon \right), \quad (3.19)$$

which is identical to (3.7).

Disconnected phase contribution To obtain the contribution from the disconnected phase, we consider the geodesic connecting one endpoint of the interval A_1 and the point $A_3(\rho_3, \tau_3, \phi_3)$ on the EOW brane (2.5). The length of this geodesic is given by

$$D_{13} = \log \left(\cos(\tau_1 - \tau_3) \cosh \rho_3 - \cos(\phi_1 - \phi_3) \sinh \rho_3 \right) - \log \epsilon, \quad (3.20)$$

where we have expanded the result with respect to ϵ . Similarly, the location of the point A_3 on the flat EOW brane is determined by the extremal condition

$$\partial_{\tau_3} D_{13} = 0, \quad \partial_{\rho_3} D_{13} = 0, \quad (3.21)$$

if the coordinate ϕ_3 is considered as a function of τ_3 and ρ_3 , as determined by (2.5). Alternatively, any two of the coordinates among (ρ_3, τ_3, ϕ_3) can be used to express the extremal condition, with the remaining coordinate regarded as a function of these two. However, any of them is hard to solve since they are transcendental equations.

To proceed, we consider the coordinate transformation of (ρ_3, τ_3, ϕ_3) to the Poincare coordinate. Or equivalently, one global coordinate and one Poincare coordinate in the embedding can be replaced into (3.2), resulting

$$D_{13} = \log \frac{\cos \tau_1 (1 - t_3^2 + x_3^2 + z_0^2) + \cos \phi_1 (-1 - t_3^2 + x_3^2 + z_0^2) + 2t_3 \sin \tau_1 - 2x_3 \sin \phi_1}{2z_0} - \log \epsilon, \quad (3.22)$$

where the point A_3 on the flat EOW $z = z_0$ is represented in the Poincare coordinate while the endpoint A_1 is represented in the global coordinate. In this case, the extremal condition to determine the location of A_3 is given by

$$\partial_{t_3} D_{13} = 0, \quad \partial_{x_3} D_{13} = 0. \quad (3.23)$$

The solution is

$$t_3 = \frac{\sin \tau_1}{\cos \tau_1 + \cos \phi_1}, \quad x_3 = \frac{\sin \phi_1}{\cos \tau_1 + \cos \phi_1}. \quad (3.24)$$

Similarly, we consider the second derivatives on the geodesic length with respect to the temporal and spatial directions

$$\partial_{t_3}^2 D_{13} < 0, \quad \partial_{x_3}^2 D_{13} > 0, \quad (3.25)$$

indicating that in the type II setup, this is also a good candidate for the disconnected geodesic since it is locally maximal with respect to temporal variations and minimal with respect to spatial variations. Then with the solution (3.24), we find the contribution to the holographic entanglement entropy from the length of the geodesic in disconnected phase

$$\begin{aligned} S_{II}^{\text{dis}} &= \frac{D_{dis,13}}{4G_N} + \frac{D_{dis,24}}{4G_N} \\ &= \frac{1}{4G_N} \left(\log \frac{z_0(\cos \tau_1 + \cos \phi_1)}{2\epsilon} + \log \frac{z_0(\cos \tau_2 + \cos \phi_2)}{2\epsilon} \right), \end{aligned} \quad (3.26)$$

where the extra contribution from the other geodesic connecting A_2 and the point on the flat EOW brane is also added. This expression of the geodesic length is the same as that in the type I case but the difference is the range of $\cos \tau_{1,2} + \cos \phi_{12}$ which is positive in the type I case and negative in the type II case. Meanwhile, we should choose the same positive sign of z_0 in both cases so that compared to the type I setup where the disconnected geodesic is space-like, in the type II setup, the disconnected

geodesic contains both time-like and space-like pieces. In summary, the disconnected geodesic in type II is found to be as follows:

$$S_{II}^{\text{dis}} = \frac{1}{4G_N} \left(\log \frac{z_0 |\cos \tau_1 + \cos \phi_1|}{2\epsilon} + \log \frac{z_0 |\cos \tau_2 + \cos \phi_2|}{2\epsilon} \right) + \frac{\pi}{2G_N} i. \quad (3.27)$$

Since this is complex valued, this should be interpreted as the pseudo entropy [44]. We argue that the final holographic (pseudo) entanglement entropy is given by selecting either S_{II}^{con} (3.19) or S_{II}^{dis} in (3.27) such that the real part is smaller.

Since the imaginary part, which comes from the time-like geodesic as discussed soon below, takes the form $\frac{\pi i}{3} c$, this may be regarded as a version of time-like entanglement entropy [45, 46]. The presence of this imaginary part show that the dual density matrix (or more properly called transition matrix) is not hermitian. Thus it is possible that the dual theory is non-unitary. In particular, since the AdS itself should be dual to a unitary CFT, this exotic feature should be due to the flat EOW brane. This suggests that the flat space gravity localized on the EOW brane is dual to a non-unitary field theory, in spite that the gravity theory in flat space is unitary, which was also implied from the fact that central charge of the dual celestial CFT is imaginary [52].

Possible profiles of Disconnected geodesic Let us study an explicit profile of the disconnected geodesic which connects the endpoint $A_1(\tau_1, \rho_\infty, \phi_1)$ of the interval and the point $A_3(\tau_3, \rho_3, \phi_3)$ (determined by (3.24) and the further coordinate transformation to the global coordinate) on the flat EOW brane. Firstly one considers the point $A'_3(\tau_3 + \pi, \rho_3, \phi_3 + \pi)$ on the flat EOW brane $z = -z_0$. Then one can find an arbitrary point $B(\tau_B, \rho_B, \phi_B)$ on the geodesic connecting A_1 and A'_3 which is space-like. There is a corresponding point $B'(\tau_B + \pi, \rho_B, \phi_B + \pi)$ on the space-like geodesic connecting $A'_1(\tau_1 + \pi, \rho_\infty, \phi_1 + \pi)$ and A_3 .

The total disconnected geodesic is then contains the following pieces: the space-like geodesic connecting A_1 and B , the time-like geodesic connecting B and B' , and also the space-like geodesic connecting B' and A_3 . We sketched in Fig.4 for the case where B coincides with A'_3 as an example.

The length of the time-like piece is

$$\cosh D_{BB'} = -1, \quad D_{BB'} = i\pi. \quad (3.28)$$

The total length of the space-like pieces is

$$D_{A_1 B} + D_{B' A_3} = D_{A_1 A'_3} = D_{A'_1 A_3} = \log \frac{-z_0 (\cos \tau_1 + \cos \phi_1)}{2\epsilon}. \quad (3.29)$$

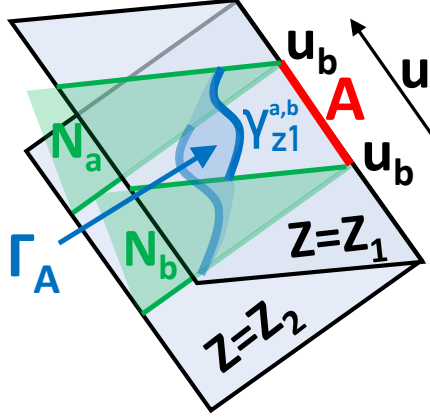


Figure 5. A sketch of calculations of holographic entanglement entropy in type III setup. The two light blue colored planes are EOW branes at $z = z_1$ and $z = z_2$, respectively, which intersects at the global AdS boundary, where we choose the subsystem A . The extremal surface which computes the entanglement entropy is Γ_A which stretches between two null surfaces N_a and N_b . This reproduces the swingle surface calculation in the flat space holography for the CCFT.

The total contribution reproduce (3.26). Among the various choices of the point B , we can choose $B = A'_3$ especially so that the total disconnected geodesic intersects with the flat EOW brane $z = z_0$ only once. This is depicted in the right panel of Fig.4.

Though the geodesic we found in this above, gives the correct geodesic length based on which we computed the holographic entanglement entropy (3.27), we have to admit that it looks like an adhoc prescription. We would like to note that a similar situation is known for the time-like entanglement entropy [45, 46], which is also given in terms of a union of time-like and space-like geodesic. It is possible that we can also have an interpretation in terms of complex geodesics as in [47, 53, 54]. We would like to leave a further study of its interpretation for a future work.

3.3 Holographic entanglement entropy in type III setup

We will then consider the holographic entanglement entropy in type III setup with the co-dimension two wedge holography. As introduced in section (2.5), there exist two flat EOW branes and the dual field theory is the CCFT_{d-1} on the null surface $|\tau + \phi| = |\tau - \phi| = \pi$ in AdS_{d+1} . The entanglement entropy is well-studied in the two dimensional CCFTs so we will consider the AdS_4 bulk ($d = 3$) in this subsection.

We consider AdS_4 in Poincare coordinate

$$ds^2 = \frac{1}{z^2}(dz^2 + ds_b^2), \quad ds_b^2 = -dt^2 + dx^2 + dy^2 = -dt^2 + dr^2 + r^2 d\Phi^2 = -du^2 - 2du dr + r^2 d\Phi^2, \quad (3.30)$$

where the last equations come from a further transformation to the coordinate (z, t, r, Φ)

$$t = u + r, \quad x = r \cos \Phi, \quad y = r \sin \Phi. \quad (3.31)$$

The point in the null boundary of the constant z slice as $r \rightarrow \infty$ becomes the point

$$\rho \rightarrow \infty, \quad \cos^2 \tau = \cos^2 \phi = \frac{u^2}{1 + u^2}, \quad \tan \theta = \tan \Phi, \quad (3.32)$$

in the global coordinate $(\rho, \tau, \phi, \theta)$

$$ds^2 = -\cosh^2 \rho d\tau^2 + d\rho^2 + \sinh^2 \rho (d\phi^2 + \sin^2 \phi d\theta^2). \quad (3.33)$$

Note that it is z -independent so that the null boundary of the slices with different z corresponds to the same null surface $\cos^2 \tau = \cos^2 \phi$, where the CCFT lives. With two flat EOW branes at $z = z_1, z_2$ inserted, the intersection is the above null surface. The interval A is considered also in this null surface, labeled by its two endpoints $A_a(u_a, \Phi_a)$ and $A_b(u_b, \Phi_b)$. We argue that the holographic entanglement entropy for the interval A is

$$S_A = \frac{\text{Area}(\Gamma_A)}{4G_N}, \quad (3.34)$$

where Γ_A is the two-dimension surface determined in the following steps:

- 1 Find the null geodesics $\gamma_z^{a,b}$ on the constant z slices, with $\partial \gamma_z^{a,b} = A_{a,b}$. The tangent vector of the null geodesics are the bulk modular flow generators on fixed z slices between the two flat EOW branes $z_1 < z < z_2$. Then they determines two null surfaces N_a, N_b which are the unions of $\gamma_z^{a,b}$ with $z_1 < z < z_2$.
- 2 Consider two arbitrary curves Γ_a, Γ_b on the null surface N_a, N_b , with the two endpoints on the two flat EOW brane $z = z_{1,2}$, parametrized by $r_{a,b}(z)$.
- 3 Find the two-dimension extremal surface Γ_A in the bulk region bounded by the two branes, with $\partial \Gamma_A = \Gamma_a \cup \Gamma_b$.
- 4 Minimize the area of Γ_A with respect to the two curves $\Gamma_{a,b}$ on the two null surfaces $N_{a,b}$.

5 The final surface which computes the entanglement entropy is given by the combination of part of $N_{a,b}$ and Γ_A . The range of $N_{a,b}$ is bounded by the curves $\Gamma_{a,b}$ found in the step 4. Since $N_{a,b}$ are null, without contribution to the area, the holographic entanglement entropy is captured by the surface Γ_A .

This is a generalization of the holographic entanglement entropy in the wedge holography [39] for the AdS branes to our flat branes. This fits nicely with the swing surface proposal in Flat₃/CCFT₂ correspondence [48, 55]. As in the swing surface proposal, the bench is described by the parametric equations

$$\begin{aligned} x &= \csc(\Phi_a - \Phi_b)((u_a - t) \sin \Phi_b + (t - u_b) \sin \Phi_a), \\ y &= -(\csc(\Phi_a - \Phi_b)((u_a - t) \cos \Phi_b + (t - u_b) \cos \Phi_a)), \end{aligned} \quad (3.35)$$

and the range of t is

$$t \in \left[\frac{u_a - u_b}{\cos(\Phi_a - \Phi_b) - 1} + u_a, \frac{u_b - u_a}{\cos(\Phi_a - \Phi_b) - 1} + u_b \right]. \quad (3.36)$$

We will verify later that (3.35) and (3.36) give also the required two-dimension surface Γ_A in AdS₄ in the Poincare coordinate (3.30).

The holographic entanglement entropy is then

$$S_A = \frac{\text{area}(\Gamma_A)}{4G} = \left(\frac{1}{z_1} - \frac{1}{z_2} \right) \frac{1}{4G} (u_a - u_b) \cot \frac{\Phi_a - \Phi_b}{2}. \quad (3.37)$$

Compared to the entanglement entropy in CCFT₂ [48, 55, 56]

$$S_A = \frac{c_L}{6} \log \left(\frac{2}{\epsilon} \sin \frac{\Phi_a - \Phi_b}{2} \right) + \frac{c_M}{12} (u_a - u_b) \cot \frac{\Phi_a - \Phi_b}{2}, \quad (3.38)$$

we have the central charges of the dual CCFT₂ in type III setup

$$c_L = 0, \quad c_M = \frac{3}{G_N} \left(\frac{1}{z_1} - \frac{1}{z_2} \right). \quad (3.39)$$

Verification of the choice of Γ_A Consider an arbitrary two-dimension surface in Poincare AdS₄ with the boundary $\Gamma_{a,b}$, parametrized by

$$x = f(t, z), \quad y = g(t, z), \quad (3.40)$$

with the boundary condition

$$x_a(z) = f(t_a, z), \quad y_a(z) = g(t_a, z), \quad x_b(z) = f(t_b, z), \quad y_b(z) = g(t_b, z), \quad (3.41)$$

where $x_{a,b}, y_{a,b}$ depend arbitrarily on z and $t_{a,b}$ is determined by $\phi = \phi_{a,b}, u = u_{a,b}$ and the coordinate transformation (3.31). The area functional is

$$\text{area} = \int dt dz \mathcal{L}, \quad (3.42)$$

where

$$\begin{aligned} \mathcal{L} = & \frac{1}{z^2} \left(\partial_z f(t, z)^2 \partial_t g(t, z)^2 - 2 \partial_t f(t, z) \partial_z f(t, z) \partial_z g(t, z) \partial_t g(t, z) \right. \\ & \left. + \partial_t f(t, z)^2 \partial_z g(t, z)^2 - \partial_z f(t, z)^2 + \partial_t f(t, z)^2 - \partial_z g(t, z)^2 + \partial_t g(t, z)^2 - 1 \right)^{\frac{1}{2}}. \end{aligned} \quad (3.43)$$

The Euler-Lagrange equation

$$\partial_f \mathcal{L} = \partial_\alpha \frac{\partial \mathcal{L}}{\partial (\partial_\alpha f)}, \quad \partial_g \mathcal{L} = \partial_\alpha \frac{\partial \mathcal{L}}{\partial (\partial_\alpha g)}, \quad (3.44)$$

gives the extremal surface condition

$$\partial_t^2 f = 0, \quad \partial_z^2 f = 0, \quad \partial_t^2 g = 0, \quad \partial_z^2 g = 0. \quad (3.45)$$

This indicates that the extremal surface is z independent and its intersections with constant z slices are geodesics in the flat spacetime. In other words, the extremal condition results in the curves $\Gamma_{a,b}$ with $\partial_z x_{a,b} = \partial_z y_{a,b} = 0$. This reduces the problem to one dimensional lower case where the minimization procedure with respect to $x_{a,b}, y_{a,b}, t_{a,b}$ (or equivalently $r_{a,b}$) is the same as that in the swing surface in Flat₃/CCFT₂ correspondence [48, 55], thus giving (3.35).

4 Holographic correlation functions

Next we would like to turn to holographic correlation functions to further explore physical properties. Basically, we can generalize the computations of correlation functions based on the bulk-boundary relation [4, 5] to our setups with flat EOW branes. We will focus on the two-point functions and one-point functions.

4.1 Two-point Functions in type I Case

Bulk two-point functions in the presence of EOW branes can be computed as in the standard AdS/CFT by imposing the appropriate boundary condition at the brane. Below we consider the simple case of a bulk scalar field φ in AdS₃ with mass m dual to

an primary operator O in the bulk of two dimensional BCFT. The conformal dimension of the dual operator O is $\Delta = 1 + \nu$, where $\nu = \sqrt{1 + m^2}$. We will first calculate the two-point function in the Euclidean Poincare coordinate, where the physical region is given by $0 < z < z_0$ in the coordinate $ds^2 = z^{-2}(dz^2 + dx_0^2 + dx_1^2)$, and then transform it to the global coordinate. We simply impose the Dirichlet boundary condition at the brane $z = z_0$:

$$\varphi(z_0) = 0. \quad (4.1)$$

After the Fourier transformation with respect to the coordinate (x_0, x_1) , the equation of motion of the scalar field can be solved generally as

$$\varphi(z) = z(\alpha I_\nu(kz) + \beta I_{-\nu}(kz)). \quad (4.2)$$

By imposing the boundary condition, we obtain

$$\alpha I_\nu(kz_0) + \beta I_{-\nu}(kz_0) = 0. \quad (4.3)$$

Since the two-point function can be found as $\langle O(k)O(-k) \rangle = \frac{B}{A}$ when the bulk scalar behaves $\varphi(z) \sim Az^{d-\Delta} + Bz^\Delta$ in $\text{AdS}_{d+1}/\text{CFT}_d$, we obtain

$$\langle O(k)O(-k) \rangle = -\frac{\Gamma(1-\nu)}{\Gamma(1+\nu)} \frac{I_\nu(kz_0)}{I_{-\nu}(kz_0)} \left(\frac{k}{2}\right)^{2\nu}. \quad (4.4)$$

By performing the Fourier transformation back to the real space, we find

$$\begin{aligned} \langle O(x_0, x_1)O(x'_0, x'_1) \rangle &= \frac{1}{2\pi} \int d^2k e^{ik(x-x')} \langle O(k)O(-k) \rangle \\ &= \frac{1}{2\pi} \int_0^\infty k dk \int_0^{2\pi} d\theta e^{ikr \cos \theta} \langle O(k)O(-k) \rangle \\ &= -\frac{\Gamma(1-\nu)}{\Gamma(1+\nu)} \int_0^\infty k dk J_0(kr) \frac{I_\nu(kz_0)}{I_{-\nu}(kz_0)} \left(\frac{k}{2}\right)^{2\nu}, \end{aligned} \quad (4.5)$$

where we set $(x_0, x_1) = (r \cos \theta, r \sin \theta)$.

On the other hand, if we impose the Neumann boundary condition at the brane $z = z_0$:

$$\varphi'(z_0) = 0, \quad (4.6)$$

then we obtain

$$\frac{\beta}{\alpha} = -\frac{I_{-\nu}(kz_0) + kz_0 I'_{-\nu}(kz_0)}{I_\nu(kz_0) + kz_0 I'_\nu(kz_0)} = \frac{(\nu+1)I_{-\nu}(kz_0) + kz_0 I_{-(\nu+1)}(kz_0)}{(\nu+1)I_\nu(kz_0) - kz_0 I_{\nu+1}(kz_0)}. \quad (4.7)$$

This leads to

$$\langle O(k) O(-k) \rangle = \frac{\Gamma(1-\nu)}{\Gamma(1+\nu)} \left(\frac{k}{2} \right)^{2\nu} \frac{I_{-\nu}(kz_0) + kz_0 I'_{-\nu}(kz_0)}{I_{\nu}(kz_0) + kz_0 I'_{\nu}(kz_0)}. \quad (4.8)$$

We can similarly obtain the real space correlation function as in (4.5).

Now, we Wick rotate (x_0, x_1) back to the Lorentzian coordinate by $x_0 = it$ and $x_1 = x$ and perform the conformal transformation:

$$t + x = \tan \frac{\tau + \phi}{2}, \quad t - x = \tan \frac{\tau - \phi}{2}, \quad (4.9)$$

where the cut off changes as

$$e^{\rho\infty} z_c = \frac{2}{\cos \tau + \cos \phi}. \quad (4.10)$$

Thus, the correlation function in the cylindrical coordinate reads

$$\langle O(\tau, \phi) O(\tau', \phi') \rangle = \frac{1}{(\cos \tau + \cos \phi)^{\Delta_+} (\cos \tau' + \cos \phi')^{\Delta_+}} \cdot \langle O(t, x) O(t', x') \rangle. \quad (4.11)$$

Note that $\langle O(t, x) O(t', x') \rangle$ can be found from the holographic result (4.5) by setting

$$r^2 = - \left(\tan \frac{\tau + \phi}{2} - \tan \frac{\tau' + \phi'}{2} \right) \left(\tan \frac{\tau - \phi}{2} - \tan \frac{\tau' - \phi'}{2} \right). \quad (4.12)$$

We can easily that in the short distance limit $r \rightarrow 0$, we find $\langle O(\tau, \phi) O(\tau', \phi') \rangle \propto r^{-2\Delta}$, which reproduces the standard result of CFT vacuum, as expected.

To explicitly calculate the behavior the two-point function (4.5), we focus on the special case $m^2 = -\frac{3}{4}$ which corresponds to $\nu = \frac{1}{2}$ below. Then, we get

$$\begin{aligned} \langle O(x_0, x_1) O(x'_0, x'_1) \rangle &= \int_0^\infty k dk J_0(kr) \cdot \frac{k(1 + e^{2kz_0})}{1 - e^{2kz_0}} \\ &= - \int_0^\infty k^2 dk \sum_{n=0}^\infty J_0(kr) (e^{-2nkz_0} + e^{-2(n+1)kz_0}) \\ &= \sum_{n=0}^\infty \left[\frac{r^2 - 8n^2 z_0^2}{(4n^2 z_0^2 + r^2)^{\frac{5}{2}}} + \frac{r^2 - 8(n+1)^2 z_0^2}{(4(n+1)^2 z_0^2 + r^2)^{\frac{5}{2}}} \right], \\ &= \sum_{n=-\infty}^\infty \left[\frac{3r^2}{(r^2 + 4n^2 z_0^2)^{\frac{5}{2}}} - \frac{2}{(r^2 + 4n^2 z_0^2)^{\frac{3}{2}}} \right]. \end{aligned} \quad (4.13)$$

First of all, it is straightforward to show the following behaviors

$$G(r) \simeq \frac{1}{r^3} \quad (r \rightarrow 0). \quad (4.14)$$

By performing the Poisson re-summation, we obtain

$$\begin{aligned}\langle O(x_0, x_1)O(x'_0, x'_1) \rangle &= \sum_{m=1}^{\infty} \left[\frac{2\pi^2}{z_0^3} m^2 K_2 \left(\frac{\pi r m}{z_0} \right) - \frac{4\pi m}{z_0^2 r} K_1 \left(\frac{\pi r m}{z_0} \right) \right] \\ &= \frac{2\pi^2}{z_0^3} \sum_{m=1}^{\infty} m^2 K_0 \left(\frac{\pi r m}{z_0} \right).\end{aligned}\quad (4.15)$$

This clearly shows the long distance behavior:

$$\langle O(x_0, x_1)O(x'_0, x'_1) \rangle \sim \frac{1}{\sqrt{r}} e^{-\frac{\pi r}{z_0}} \quad (4.16)$$

in the limit $r \rightarrow \infty$.

Now we turn to the behavior the two-point function in the diamond coordinate (τ, ϕ) . In particular, consider the limit where the location of one of the operators gets closer to the boundary $\cos \tau + \cos \phi = 0$ of the diamond. In our type I case, this boundary is acutual BCFT boundary. We note that the conformal factor (4.11) gets divergent at the boundary. However, $\langle O(x_0, x_1)O(x'_0, x'_1) \rangle$ as long as $x - x'$ is space-like, shows the exponential decay (4.16) when (τ, ϕ) approaches the boundary i.e. $r \rightarrow \infty$. Thus, the two-point function $\langle O(\tau, \phi)O(\tau', \phi') \rangle$ on the diamond gets vanishing in this limit. This means that the operator becomes trivial when it is moved to the null boundary and implied that the null boundary looks like a final state projection, which removes the degrees of freedom.

As a consistency check, let us compare this with the case where there is no physical boundary along the diamond, where we always have $\langle O(x_0, x_1)O(x'_0, x'_1) \rangle \propto r^{-2\Delta}$ and this leads

$$\langle O(\tau, \phi)O(\tau', \phi') \rangle_{\text{vacuum}} = \frac{1}{(\cos(\tau - \tau') - \cos(\phi - \phi'))^{\Delta_+}}, \quad (4.17)$$

which has no special behavior at the edge of diamond as opposed to our type I BCFT case and coincides with the standard result of a CFT vacuum on a cylinder.

4.2 Two-point functions in type II Case

Next, we address the two-point functions in the type II case. It is more convenient to perform the calculations in Poincare coordinates, where the boundary conditions are simpler. Note that the embedding (2.3) is valid for both $z > 0$ and $z < 0$, with the two regions separated by the surface $X_0 = X_2$, corresponding to $z \rightarrow \pm\infty$. In the type

II setup, we can place the flat EOW brane at $z = z_0 < 0$ in the negative z region and examine the asymptotic behavior of the bulk scalar as $z \rightarrow 0^+$. The physical region of interest is defined by $\{0 < z < +\infty\} \cap \{-\infty < z < z_0\}$. The basic approach is as follows: first, we determine the scalar solution in the region $-\infty < z < z_0$ by imposing the boundary condition on the flat EOW brane at $z = z_0$. Then, we consider the matching condition at $z \rightarrow \pm\infty$ to determine the solution in the region $0 < z < +\infty$.

Either Dirichlet boundary condition $\varphi_-(z_0) = 0$ or Neumann boundary condition $\varphi'_-(z_0) = 0$ can be imposed. The solution in the momentum space is in general labeled as

$$\varphi_-(z) = z(\alpha_- I_\nu(kz) + \beta_- I_{-\nu}(kz)), \quad (4.18)$$

where the coefficients are specified as α_-, β_- since this the solution $\varphi_-(z)$ valid for the region $-\infty < z < z_0$.

Then, we want to determine the matching condition at $z \rightarrow \pm\infty$. Note that the interior of the surface $X_0 = X_2$ is covered by the limit [57]

$$z \rightarrow \pm\infty, \quad z^2 + r^2 = \frac{a}{2}z, \quad x^2 = b^2 z^2, \quad r^2 = x^2 - t^2, \quad (4.19)$$

in Poincare coordinate, related to the global coordinate by

$$\sec \rho = \sqrt{1 + a^2 + b^2}, \quad \cos \tau = \frac{a}{\sqrt{1 + a^2 + b^2}}, \quad \sin \phi = \frac{a}{\sqrt{a^2 + b^2}}. \quad (4.20)$$

Then, we perform the Fourier transformation on the solution to go back to the real space

$$\varphi_{-,+}(z, r) = \frac{1}{2\pi} \int_0^\infty k dk \int_0^{2\pi} d\theta e^{ikr \cos \theta} \varphi_{-,+}(z) = \int_0^\infty k dk J_0(kr) \varphi_{-,+}(z), \quad (4.21)$$

where φ_+ labels the solution in the region $0 < z < +\infty$

$$\varphi_+(z) = z(\alpha_+ I_\nu(kz) + \beta_+ I_{-\nu}(kz)), \quad (4.22)$$

where the coefficients are labeled as α_+, β_+ . We impose the matching condition formally

$$\lim_{z \rightarrow +\infty} \varphi_+(z, r)|_{z^2 + r^2 = \frac{a}{2}z} = \lim_{z \rightarrow -\infty} \varphi_-(z, r)|_{z^2 + r^2 = \frac{a}{2}z}. \quad (4.23)$$

In the limit (4.19),

$$\varphi_{-,+} \rightarrow \int_0^\infty k dk I_0(-kz + \frac{ak}{4}) z(\alpha_{-,+} I_\nu(kz) + \beta_{-,+} I_{-\nu}(kz)). \quad (4.24)$$

With the large z behavior of $I_\nu(z)$ for fixed ν ,

$$I_\nu(z) \sim \begin{cases} \frac{e^z}{\sqrt{2\pi z}}, & |\arg z| < \frac{1}{2}\pi - \delta, \\ \frac{e^{-z+(\nu+\frac{1}{2})\pi i}}{\sqrt{2\pi z}}, & \frac{1}{2}\pi + \delta < \pm \arg z < \frac{3}{2}\pi - \delta, \end{cases} \quad (4.25)$$

Since the solutions (4.21) get divergent exponentially as $z \rightarrow \pm\infty$, we should expand the solutions in terms of z at $z \rightarrow \pm\infty$ and match the coefficients of the divergent term and the constant term, leading to

$$\alpha_+ = -\alpha_- e^{8ak-i\pi v}, \quad \beta_+ = -\beta_- e^{8ak+i\pi v}. \quad (4.26)$$

Note that the ratio $\frac{\beta_{-,+}}{\alpha_{-,+}}$ is k -independent, so that we find the relation between the two-point function $\langle O(t, x)O(t', x') \rangle_{II}$ in the type II case and that $\langle O(t, x)O(t', x') \rangle_I$ in the type I case

$$\langle O(t, x)O(t', x') \rangle_{II} = e^{2\pi i \nu} \langle O(t, x)O(t', x') \rangle_I. \quad (4.27)$$

The difference is only the overall phase factor $e^{2\pi i \nu}$. We can then go to the cylindrical coordinate where this overall phase factor cancels the signs in the conformal factor $(\cos \tau + \cos \phi)^{\Delta+} (\cos \tau' + \cos \phi')^{\Delta+}$ and get

$$\langle O(\tau, \phi)O(\tau', \phi') \rangle_{II} = \langle O(\tau, \phi)O(\tau', \phi') \rangle_I. \quad (4.28)$$

4.3 One-point functions in type I and II case

We will calculate the one-point functions in the type I and II setups in this subsection. To have a non-vanishing one-point function in the AdS/BCFT as considered in [19, 31], the source term is added on the EOW brane

$$I_s = -\frac{a}{8\pi G} \int_{EOW} \sqrt{|h|} \phi, \quad (4.29)$$

where h is the determinant of the induced metric on the EOW brane and a is the coupling constant. In this case, the holographic one-point function on the asymptotic boundary can be derived using the bulk-to-boundary propagator as follows [31, 32, 58]:

$$\langle O(x) \rangle = a \cdot \int_{EOW} d^2 x_b \sqrt{|h|} K_{Bb}^\Delta(x; x_b). \quad (4.30)$$

where the coordinates x and x_b denote the two points on the asymptotic boundary and the EOW brane, respectively and $K_{Bb}^\Delta(x; x_b)$ is the bulk-to-boundary propagator with

the EOW brane for the scalar operator with conformal dimension Δ . It can be related to the bulk-to-bulk propagator in AdS_3 without the EOW brane[5, 59, 60]

$$G_{\text{bulk-bulk}}(x, x') = \frac{\Gamma(\Delta)}{2^{\Delta+1}(\Delta-1)\pi\Gamma(\Delta-1)} \xi^\Delta \cdot {}_2F_1\left(\frac{\Delta}{2}, \frac{\Delta+1}{2}; \Delta-; \xi^2\right), \quad (4.31)$$

where we have introduced the chordal distance ξ that is associated with the geodesic distance $D(x, x')$

$$D(x; x') = \ln\left(\frac{1 + \sqrt{1 - \xi^2}}{\xi}\right), \quad \xi = \frac{1}{\cosh(D(x; x'))}. \quad (4.32)$$

The bulk-to-bulk propagator satisfies the equation

$$(\square_G + m^2) G_{\text{BB}}^\Delta(x; x') = \frac{\delta^{(d+1)}(x - x')}{\sqrt{G}}, \quad (4.33)$$

where \square_G is the scalar Laplacian operator in AdS spacetime and the mass of the bulk field is related to the conformal dimension of the dual operator on the boundary via the standard AdS/CFT dictionary $m^2 = \Delta(\Delta - 2)$.

In the presence of a flat EOW brane, the bulk-to-bulk propagator can be calculated using the method of images, with the brane acting as a mirror. The Dirichlet or Neumann boundary conditions on this brane can be replicated by introducing an additional source in the equation (4.33), positioned according to the reflection of the brane. Additionally, the background AdS spacetime must also be reflected by this brane. Thus, the bulk-to-bulk propagator with the flat EOW brane is

$$G_{\text{EOW}}(x, x') = G_{\text{BB}}(x, x') \pm \tilde{G}_{\text{BB}}(x, Rx') \quad (4.34)$$

where $\tilde{G}_{\text{BB}}(x, Rx')$ is calculated in the glued AdS geometry via the EOW brane and Rx' is the location of the image of x' . The sign \pm is suitable for Neumann and Dirichlet boundary condition. Specially, if one of the bulk point is on the EOW brane,

$$\tilde{G}_{\text{BB}}(x, Rx')|_{x' \in \text{EOW}} = G_{\text{BB}}(x, x')|_{x' \in \text{EOW}}. \quad (4.35)$$

So only the Neumann boundary condition leads to non-vanishing bulk-to-bulk propagator with the flat EOW brane, if one of the bulk point is on the brane,

$$G_{\text{EOW}}(x, x')|_{x' \in \text{EOW}} = 2G_{\text{BB}}(x, x')|_{x' \in \text{EOW}} \quad (4.36)$$

Then, the bulk-to-boundary propagator with the EOW brane appearing in (4.30) $K_{\text{Bb}}^\Delta(x; x_b)$ can be derived by taking the boundary limit of the bulk-to-bulk propagator (4.36) with the flat EOW brane. For example, in the Poincare coordinate, we have

$$K_{\text{Bb}}^\Delta(x; x_b) = 2 \lim_{z \rightarrow 0} \frac{2\Delta - 2}{z^\Delta} G_{\text{EOW}}(x, x_b)|_{x_b \in \text{EOW}}. \quad (4.37)$$

The bulk-to-boundary propagator in other coordinates is obtained from the coordinate transformations.

We then consider the large Δ limit of these operators, since the disconnected phase contribution to the holographic entanglement entropy is related to the one-point function of the twist operator with large Δ . By taking $\Delta \rightarrow \infty$, we can approximate the bulk-to-bulk propagator and by the geodesic distance [61],

$$G_{BB}(x, x') = \frac{1}{2\Delta - 2} e^{-\Delta D(x; x')} \left(\frac{\Delta}{2\pi} \frac{1 + \sqrt{1 - \xi^2}}{\sqrt{1 - \xi^2}} \right), \quad (4.38)$$

resulting the bulk-to-boundary propagator with the flat EOW brane in the Poincare coordinate,

$$K_{\text{Bb}}^\Delta(x; x_b) = 2 \frac{\Delta}{\pi} \left(\frac{z_0}{z_0^2 + (x - x_b)^2 - (t - t_b)^2} \right)^\Delta. \quad (4.39)$$

Type I setup In this case, the brane is located at $z = |z_0| > 0$. In the Poincare patch, equations (4.30), (4.39) can be used directly to calculate the holographic one-point function with large Δ ,

$$\langle O(x) \rangle_I = 2a \int dx_b dt_b \frac{\Delta}{\pi z_0^2} \left(\frac{z_0}{z_0^2 + (x - x')^2 - (t - t_b)^2} \right)^\Delta = \frac{a\Delta}{|z_0|^\Delta}. \quad (4.40)$$

In the global coordinate, it is more convenient to use the geodesic length with one global coordinate and one Poincare coordinate, e.g. (3.22), in the geodesic length approximation,

$$K_{\text{Bb}}^\Delta(x; x_b) = 2e^{-\Delta D_{13}(x; x_b)} \left(\frac{\Delta}{\pi} \right), \quad (4.41)$$

leading to

$$\langle O(x) \rangle_I = 2a \int dx_b dt_b \frac{1}{z_0^2} K_{\text{Bb}}^\Delta(x; x_b) = a\Delta \left(\frac{2}{|z_0|(\cos \tau + \cos \phi)} \right)^\Delta. \quad (4.42)$$

This is consistent with the result via the plane-to-cylinder conformal map and the Poincare coordinate calculation (4.40), serving as the consistency check of the validity of the chordal distance method to get the geodesic with one global coordinate and one Poincare coordinate.

Type II setup In this case, the flat EOW brane is located at $z = -|z_0| < 0$. For large Δ , the geodesic length (3.22) can be exploited to get

$$\langle O(x) \rangle_{II} = 2a \int dx_b dt_b \frac{1}{z_0^2} K_{\text{Bb}}^\Delta(x; x_b) = a\Delta \left(\frac{2}{-|z_0|(\cos \tau + \cos \phi)} \right)^\Delta. \quad (4.43)$$

Compared to the type I setup with the brane at $z = |z_0|$, there is an overall phase factor in the one-point function $e^{\pi i \Delta}$, which is consistent with the phase factor in front of the two-point function $e^{2\pi i \nu} = e^{2\pi i \Delta}$.

Saddle point approximation and disconnected phase contribution to holographic entanglement entropy Note that the integration (4.40), (4.43) above to get the one-point function can also be calculated by the saddle point approximation, with the saddle point

$$x_b = x, \quad t_b = t, \quad (4.44)$$

in the Poincare coordinate calculation and

$$t_b = \frac{\sin \tau}{\cos \tau + \cos \phi}, \quad x_b = \frac{\sin \phi}{\cos \tau + \cos \phi}, \quad (4.45)$$

in the one Poincare coordinate and one global coordinate calculation. They are actually the same saddle point as (3.11), (3.24) in the disconnected phase contribution to the holographic entanglement entropy. From the BCFT point of view, the entanglement entropy can be derived from the two-point function of the twist operator,

$$S_{\mathcal{A}} \equiv \lim_{n \rightarrow 1} \frac{1}{1-n} \log \langle \sigma_n(A_1) \bar{\sigma}_n(A_2) \rangle, \quad (4.46)$$

where the normalization of twist operators is fixed as $\langle \sigma_1(A_1) \bar{\sigma}_1(A_2) \rangle = 1$ and their conformal dimension is $\Delta_n = \frac{c}{12} (n - \frac{1}{n})$. In the semi-classical limit of a holographic field theory, this is equivalent to taking a large central charge limit $\Delta_n \sim c \sim \frac{1}{G_N} \rightarrow \infty$. For a holographic BCFT, the two-point functions at leading order in the large central charge limit $c \rightarrow \infty$ are dominated by two distinct channels

$$\langle \sigma_n(A_1) \bar{\sigma}_n(A_2) \rangle_{\text{BCFT}} = \max \begin{cases} \langle \sigma_n(A_1) \bar{\sigma}_n(A_2) \rangle \\ \langle \sigma_n(A_1) \rangle \langle \bar{\sigma}_n(A_2) \rangle \end{cases}. \quad (4.47)$$

Here, the one-point function is non-vanishing due to the presence of a boundary in the background. These two channels correspond to the connected and disconnected phase

contributions to the holographic entanglement entropy. In the disconnected phase, the one-point function of the twist operator with large Δ can be calculated by the saddle point approximation above

$$\langle \sigma_n(A) \rangle \sim \sqrt{\frac{|h|}{\det(D''(x_A; x_b^*))}} e^{-\Delta_n D(x_A; x_b^*)} = e^{-\Delta_n D(x_A; x_b^*)}, \quad (4.48)$$

leading to the contribution to the holographic entanglement entropy from the disconnected geodesics

$$\begin{aligned} S_A &\approx \lim_{n \rightarrow 1} \frac{1}{1-n} \left(\lim_{\Delta_n \rightarrow \infty} (\log \langle \sigma_n(A_1) \rangle + \log \langle \sigma_n(A_2) \rangle) \right) \\ &= \frac{c}{6} (D_{13} + D_{24}), \end{aligned} \quad (4.49)$$

where the point A_3, A_4 on the flat EOW brane is determined by the saddle point. Note that this is similar to the usual $\text{AdS}_3/\text{BCFT}_2$ correspondence with an AdS brane, where the equivalence between (4.47) and the holographic entanglement entropy formula can be demonstrated using the geodesic approximation and different from the dS EOW brane case [41], where the saddle point is not stable.

4.4 Type III Case

Finally, we turn to the type III case. In the Poincare coordinate, the gravity dual is situated in the region $z_1 < z < z_2$ surrounded by the two EOW branes. Consider a free massive scalar φ in the type III geometry. In the metric (2.2), the equation of motion reads

$$z^{d+1} \partial_z (z^{1-d} \partial_z \varphi) + z^2 (-\partial_t^2 + \partial_{\vec{x}}^2) \varphi - m^2 R^2 \varphi = 0. \quad (4.50)$$

The Fourier transformation

$$\varphi(t, x, z) = \psi(z) e^{-i\omega t + i\vec{k} \cdot \vec{x}}, \quad q^2 \equiv \omega^2 - k^2, \quad (4.51)$$

leads to the radial ODE

$$z^2 \psi''(z) - (d-1)z\psi'(z) + (q^2 z^2 - m^2 R^2) \psi(z) = 0. \quad (4.52)$$

The above is the Bessel equation of order $\nu = \sqrt{(\frac{d}{2})^2 + m^2 R^2}$. Its general solution takes the form:

$$\psi(z) = z^{d/2} [AJ_\nu(qz) + BY_\nu(qz)]. \quad (4.53)$$

We impose Neumann conditions on the scalar at $z = z_1$ and $z = z_2$:

$$\psi'(z_1) = 0, \quad \psi'(z_2) = 0. \quad (4.54)$$

Define the shorthand

$$F_d(x) \equiv \frac{d}{2} J_\nu(x) + x J'_\nu(x), \quad G_d(x) \equiv \frac{d}{2} Y_\nu(x) + x Y'_\nu(x). \quad (4.55)$$

Then, the general solution can be obtained:

$$\psi'(z) = z^{\frac{d-2}{2}} [A F_d(qz) + B G_d(qz)]. \quad (4.56)$$

The Neumann conditions at $z = z_1$ and $z = z_2$ give a homogeneous linear system

$$\begin{pmatrix} F_d(qz_1) & G_d(qz_1) \\ F_d(qz_2) & G_d(qz_2) \end{pmatrix} \begin{pmatrix} A \\ B \end{pmatrix} = 0, \quad (4.57)$$

which admits a nontrivial solution only if its determinant vanishes:

$$F_d(qz_1) G_d(qz_2) - G_d(qz_1) F_d(qz_2) = 0. \quad (4.58)$$

This is the quantization condition determining the discrete spectrum $q = q_n$.

A convenient choice of coefficients that automatically satisfies $\psi'(z_1) = 0$ is

$$A = G_d(q_n z_1), \quad B = -F_d(q_n z_1). \quad (4.59)$$

Thus, the properly modes are

$$\psi_n(z) = z^{\frac{d-2}{2}} \left[J_\nu(q_n z) G_d(q_n z_1) - Y_\nu(q_n z) F_d(q_n z_1) \right], \quad (4.60)$$

and one checks directly that $\psi'_n(z_1) = \psi'_n(z_2) = 0$.

This calculation shows that we can view the scalar field in the $d + 1$ dimensional bulk as the tower of infinitely many scalar field with various masses q_n^2 in d dimensional flat space $\mathbb{R}^{1,d-1}$, as we can find from (4.51). Thus, the analysis of the correlations functions will essentially become the same as that in the flat spacetime holography [14, 62–64]. We leave its detailed analysis for a future work. Instead, below we will see how the spectrum looks like in a few examples.

$d = 3$ (**AdS₄**) **case** We set $d = 3$ and $m^2 = 0$, namely $\nu = \frac{3}{2}$. The Neumann boundary conditions at $z = z_1, z_2$ are built from

$$F_3(x) = \frac{3}{2}J_{\frac{3}{2}}(x) + xJ'_{\frac{3}{2}}(x), \quad G_3(x) = \frac{3}{2}Y_{\frac{3}{2}}(x) + xY'_{\frac{3}{2}}(x). \quad (4.61)$$

Using the Bessel identity $xJ'_\nu + \nu J_\nu = xJ_{\nu-1}$ (and the same for Y_ν), one immediately finds

$$F_3(x) = xJ_{\frac{1}{2}}(x), \quad G_3(x) = xY_{\frac{1}{2}}(x). \quad (4.62)$$

Therefore, the quantization condition can be written as

$$J_{\frac{1}{2}}(qz_1)Y_{\frac{1}{2}}(qz_2) - Y_{\frac{1}{2}}(qz_1)J_{\frac{1}{2}}(qz_2) = 0. \quad (4.63)$$

For half-integer order, the Bessel functions admit closed forms

$$J_{\frac{1}{2}}(x) = \sqrt{\frac{2}{\pi x}} \sin x, \quad Y_{\frac{1}{2}}(x) = -\sqrt{\frac{2}{\pi x}} \cos x \quad (4.64)$$

and all common prefactors cancel out in the determinant.

$$-\sin(qz_1)\cos(qz_2) + \cos(qz_1)\sin(qz_2) = \sin(q(z_2 - z_1)) = 0. \quad (4.65)$$

Writing $L \equiv z_2 - z_1 > 0$, the spectrum is thus

$$q_n = \frac{n\pi}{L} \quad (n \in \mathbb{Z}). \quad (4.66)$$

$d = 2$ (**AdS₃**) **case** We set $d = 2$ and $m^2 = -\frac{3}{4}$, namely $\nu = \frac{1}{2}$. Proceeding as above and using the half-integer closed forms for $J_{1/2}, Y_{1/2}$, the quantization condition reduces exactly to

$$\left(q^2 z_1 z_2 + \frac{1}{4}\right) \sin(qL) + \frac{1}{2}qL \cos(qL) = 0 \quad (4.67)$$

Equivalently,

$$\tan qL = -\frac{\frac{1}{2}qL}{q^2 z_1 z_2 + \frac{1}{4}} \quad (4.68)$$

The solution of this equation for $n \gg 1$ is given as follows:

$$q_n = \frac{n\pi}{L} - \frac{L}{2z_1 z_2 n\pi} + O\left(\frac{1}{n^3}\right). \quad (4.69)$$

5 On-shell action in Euclidean Poincare AdS₃

In this section, we will calculate the Euclidean on-shell action of Einstein gravity in AdS₃ ($d = 2$), which is expected to be equal to the partition function (or free energy) of the dual field theory. The starting point is the Euclidean Poincare AdS₃,

$$ds^2 = \frac{dt_E^2 + dx^2 + dz^2}{z^2}, \quad (5.1)$$

with the EOW brane

$$z = z_0. \quad (5.2)$$

The Euclidean on-shell action is

$$I_E = -\frac{1}{16\pi G_N} \int_M \sqrt{g}(\mathcal{R} - 2\Lambda) - \frac{1}{8\pi G_N} \int_Q \sqrt{h}(K - T), \quad (5.3)$$

where G_N is the three-dimensional gravitational constant. The first term represents the Einstein-Hilbert term calculated in the bulk, specifically within the region (2.8) defined in AdS₃. The second term corresponds to the Gibbons-Hawking terms evaluated on the boundary, which includes the surfaces at $z = 0$ and $z = z_0$ in the type I case, and the brane at $z = z_0$ in the type II case. Besides, the brane tension term is considered to give the proper EOW brane equation of motion (2.1). Below we will mainly focus on the type I case as a similar result can also be obtained for type II by flipping the sign. Below we will give two different prescriptions to regulate the UV and IR divergences, which eventually gives the same on-shell action.

5.1 Regularization by deforming the cut off surface

Direct calculations encounter divergences from the $z = z_0$ surface, representing the UV divergence typical in calculations involving the asymptotic boundary of AdS, as well as an additional IR divergence as t_E, x approach infinity. To address these issues, it is crucial to introduce a cutoff surface to regulate both types of divergences. Subsequently, we calculate the action (5.3) within the region bounded by the EOW brane at $z = z_0$ and the cutoff surface.

We deform the cut off surface into the form

$$r^2 + \left(z - \frac{1}{\epsilon} - \epsilon\right)^2 = \frac{1}{\epsilon^2}, \quad (5.4)$$

to regulate the IR divergence, where

$$r^2 = x^2 + t_E^2. \quad (5.5)$$

and ϵ is a small parameter. This surface is a very large semi-sphere with radius $\frac{1}{\epsilon}$, whose center is located at

$$z = \epsilon + \frac{1}{\epsilon}, \quad x = t_E = 0. \quad (5.6)$$

It intersects with $z = \text{const.}$ slices at circles with $r^2 = -\frac{(\epsilon-z)(\epsilon^2-\epsilon z+2)}{\epsilon} \rightarrow \frac{2z}{\epsilon}$ so that it regulate the IR divergence. As $\epsilon \rightarrow 0$, the cutoff surface becomes the usual cutoff surface

$$z = \epsilon, \quad (5.7)$$

so that it regulate the UV divergence from $z = 0$ at the same time. Then, we calculate the on-shell action in the region bounded by the EOW brane and the cutoff surface,

$$I_E = \frac{(\epsilon^2 + 1)(z_0 - \epsilon) + z_0 \epsilon^2 (\log \epsilon - \log z_0)}{4G_N \epsilon^2}, \quad (5.8)$$

where the contribution from the Gibbons-Hawking term on the cutoff surface is also included whose trace of the extrinsic curvature is $K_\epsilon = 2(1 + \epsilon^2)$.

We can further subtract the leading $\frac{1}{\epsilon^2}$ and subleading $\frac{1}{\epsilon}$ divergence by further adding the counter term in the gravitational action (5.3),

$$I_{ct} = \frac{1}{8\pi G_N} \int_\epsilon \sqrt{h_\epsilon} \left(1 - \frac{\mathcal{R}_\epsilon}{4} \log \epsilon \right). \quad (5.9)$$

This is the usual counter term to cancel the divergence, calculated on the cutoff surface where h_ϵ is the induced metric on the cutoff surface and \mathcal{R}_ϵ is Ricci scalar of this surface which vanishes as $\epsilon \rightarrow 0$. For the surface (5.4), the counter term reads

$$I_{ct} = -\frac{(\epsilon^2 + 1)(z_0 - \epsilon)}{4G_N z_0 \epsilon^2}, \quad (5.10)$$

leading to the total on-shell action in the type I:

$$I_{tot,I} = I_E + I_{ct} = -\frac{1}{4G_N} \log \frac{z_0}{\epsilon}. \quad (5.11)$$

What we left is the $\log \epsilon$ divergence only, similar to the usual calculation in pure AdS_3 .

We also find the total on-shell action in the type II case as

$$I_{tot} = -\frac{1}{4G_N} \log \frac{z_0}{\epsilon}. \quad (5.12)$$

This is found just by flipping the sign of the type I result because the bulk region of type II is the complement of that of type I.

5.2 Regularization by deforming flat EOW branes to AdS ones

We can also consider another regularization to get the on-shell action in type I configuration. Note that the flat EOW brane can be regarded as the limit from the AdS EOW brane,

$$t_E^2 + x^2 + (z + r_0 - z_0)^2 = r_0^2, \quad r_0 > \frac{z_0}{2}, \quad (5.13)$$

with the Ricci scalar

$$R = \frac{2z_0(z_0 - 2r_0)}{r_0^2}, \quad (5.14)$$

and the trace of the extrinsic curvature

$$K = 2T = -2 + \frac{2z_0}{r_0}. \quad (5.15)$$

As the limit $r_0 \rightarrow \infty$, it recovers the flat EOW brane $z = z_0$. In this case, the cutoff surface is imposed at $z = \epsilon$ as usual. A parallel calculation is carried out resulting

$$I_E = \frac{1}{4G_N} \left(\frac{2r_0 z_0 - z_0^2}{2\epsilon^2} + \frac{z_0 - r_0}{\epsilon} - \log \left(\frac{z_0}{\epsilon} \right) - \frac{1}{2} \right). \quad (5.16)$$

Firstly, the divergence as $z \rightarrow 0$ is regulated by setting $z = \epsilon$. Secondly, the divergence due to the $r_0 \rightarrow \infty$ limit for a fixed z_0 , which corresponds to the IR divergence, is also present. Furthermore, the bulk divergence is $\frac{1}{\epsilon^2}$, while the boundary term contributes $\frac{1}{\epsilon}$.

We should subtract the divergence with the additional counter term in the action calculated at $z = \epsilon$

$$I_{ct} = \frac{1}{4G_N} \left(-\frac{r_b^2}{2\epsilon^2} - \frac{z_0^2 - r_b^2}{2z_0\epsilon} + \frac{1}{2} \right). \quad (5.17)$$

where r_b is the radius of circle

$$r_b^2 \equiv \tau^2 + x^2 = 2r_0 z_0 - z_0^2 \quad (5.18)$$

which is the intersection between the AdS brane (5.13) and the asymptotic boundary $z = 0$. Then

$$I_{tot,I} = -\frac{1}{4G_N} \log \frac{z_0}{\epsilon}. \quad (5.19)$$

This gives the same result as (5.11) from the flat EOW brane directly and the cutoff surface (5.4), serving as a consistency check.

5.3 Comparison with boundary entropy

For AdS EOW branes [18, 19], the boundary entropy (or g -function) is related to its tension via:

$$\log g = \frac{c}{6} \log \sqrt{\frac{1+T}{1-T}}. \quad (5.20)$$

For the tensionless AdS EOW brane $T = 0$, we have $\log g = 0$, which corresponds to $r_b = z_0$ (or equally $r_0 = z_0$) in (5.13). On the other hand, in the type I (and type II) flat EOW brane limit $T = -1$ (and $T = 1$) we have $\log g = -\infty$ (and $\log g = \infty$). Since this g function is defined as the regularized disk partition function, $-\log g$ should coincide with the regularized on-shell action in the gravity.

In our calculation based the AdS brane (5.13), we can regularize the UV divergence as

$$I_{ren,I} = I_{tot,I} - I_{disk(0)} = -\frac{1}{4G_N} \log \frac{z_0}{r_b}, \quad (5.21)$$

where the $I_{disk(0)}$ is the contribution from the un-regularized disk partition function for $T = 0$ at the radius r_b , given by $I_{disk(0)} = -\frac{1}{4G_N} \log \frac{r_b}{\epsilon}$.

In the actual type I setup, we need to take the limit $r_b \rightarrow \infty$ and this leads to $I_{ren,I} = \infty$. Similar we obtain $I_{ren,II} = -\infty$. Indeed, they agree with the expected behaviors of $\log g$ (5.20) in $T = -1$ and $T = 1$ limit, respectively.

6 Euclidean Holography

Finally let us turn to a possible holographic interpretation of the Euclidean setup of the AdS/BCFT with a flat EOW brane. As we noted in section 2, the EOW brane (2.7) in the Euclidean global AdS_{d+1} intersects with the AdS boundary $\rho \rightarrow \infty$ only at a point $\phi = \pi$ and $\tau_E = 0$. We will focus on the type II setup as illustrated in Fig.6.

6.1 Holographic Setup

In this setup, the d dimensional gravity on a Euclidean flat space on the brane $z = z_0$ together with the $d+1$ bulk gravity in the region surrounded by the brane, is expected to be equivalent to a certain large N theory localized on the point $\phi = \pi$ and $\tau_E = 0$. If we introduce the UV cut off $\rho \leq \rho_\infty$, then the dual large N theory lives on a tiny region given by a d dimensional round ball, given by

$$\tau_E^2 + (\pi - \phi)^2 \leq \frac{4R}{z_0} e^{-\rho_\infty}, \quad (6.1)$$

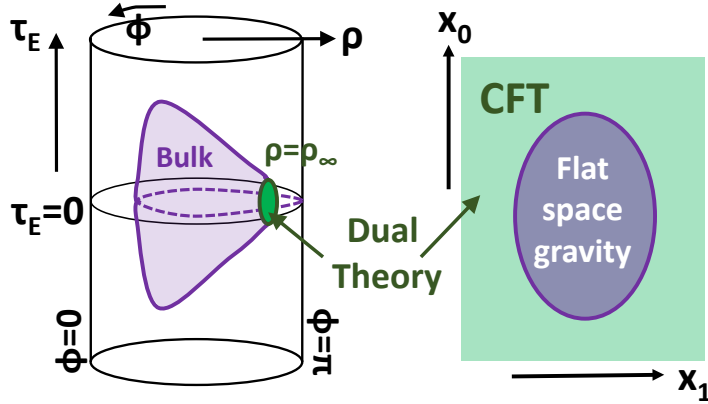


Figure 6. A sketch of Euclid type II set up with a UV cut off (left) and its dual field theory description via the double holography (right) in the Poincare coordinate.

on the cut off boundary $\rho = \rho_\infty$ of the global AdS_{d+1} . Refer to the left panel of Fig.6 for a sketch.

If we focus on the d dimensional flat space gravity realized on the brane, this is dual to the $d - 1$ dimensional boundary of the ball region (6.1). In this way, by embedding the flat brane inside AdS , we can find an explicit example of holography for gravity on a flat Euclidean space.

In terms of the Poincare AdS (2.2), the flat EOW brane has the UV cut off as

$$(R^2 + z^2 + x^2 + x_0^2)^2 - 4R^2 x_0^2 \leq 4R^2 z^2 \cosh^2 \rho_\infty, \quad (6.2)$$

with z set as $z = z_0$, where $x_0 = it$ is the Euclidean time coordinate. As in the right panel of Fig.6, there is a flat space gravity in the above region (6.2) in the dual field theory via the double holography, coupled to the CFT situated outside.

6.2 On-shell action

Since there is no space and time in the dual theory, we would like to compute its partition function by evaluating the gravity on-shell action below as the only physical quantity. Notice that this calculation is different from the one in the previous section. Here we now impose the UV cut off $\rho \leq \rho_\infty$ in the global AdS to examine the leading UV divergent contributions, while in the previous section we wanted to extract the boundary entropy contribution in the Poincare patch.

The gravity action is given by (5.3). In the current type II setup, we have

$$\begin{aligned}\mathcal{R} &= -\frac{d(d+1)}{R^2}, \quad \Lambda = -\frac{d(d-1)}{2R^2}, \\ K &= \frac{d}{R}, \quad T = \frac{d-1}{R}.\end{aligned}\tag{6.3}$$

Thus, we can write it as

$$I_E = \frac{d}{8\pi G_N R^2} \int_{M_{d+1}} \sqrt{g} - \frac{1}{8\pi G_N R} \int_{Q_d} \sqrt{h}.\tag{6.4}$$

To evaluate this in the Poincare coordinate, let us define $V(z)$ to be the volume of the regions $(x_0, x_1, \dots, x_{d-1})$ which satisfy (6.2) for a fixed value of z . In the presence of the UV cut off $\rho \leq \rho_\infty$, the coordinate z in the gravity dual takes the values $z_0 \leq z \leq Re^{\rho_\infty}$. Thus, I_E is expressed as

$$I_E = \frac{d}{8\pi G_N R} \int_{z_0}^{Re^{\rho_\infty}} dz \frac{V(z)}{z} - \frac{V(z_0)}{8\pi G_N R}.\tag{6.5}$$

The function $V(z)$ is evaluated as

$$V(z) = V_{d-2} \int_0^{x_0^{max}} dx_0 \int_0^{r^{max}(x_0)} r^{d-2} dr,\tag{6.6}$$

where V_{d-2} is the volume of the unit $d-2$ dimensional sphere and we introduced

$$\begin{aligned}x_0^{max} &= \sqrt{R^2 + 2Rz \sinh \rho_\infty - z^2}, \\ r^{max}(x_0) &= \sqrt{-(x_0^2 + R^2 + z^2) + 2R\sqrt{x_0^2 + z^2} \cosh \rho_\infty}.\end{aligned}\tag{6.7}$$

In the UV limit $\rho_\infty \rightarrow \infty$, we can approximate x^{max} and r^{max} so that they are on the d dimensional round disk:

$$(x^{max})^2 + (r^{max})^2 \leq Rze^{\rho_\infty},\tag{6.8}$$

This lead to the following estimation:

$$V(z) \simeq \frac{V_{d-1}}{d} R^{\frac{3}{2}d} z^{-\frac{d}{2}} e^{\frac{d}{2}\rho_\infty}.\tag{6.9}$$

Finally, we can evaluate the on-shell action as

$$I_E = \frac{R^{d-1}}{8\pi d G_N} \left(\frac{R}{z_0} \right)^{\frac{d}{2}} e^{\frac{d}{2}\rho_\infty} + \dots,\tag{6.10}$$

where the omitted terms are in the higher order with respect to the UV cut off.

In the standard holographic interpretation of the global AdS, the UV cut off ϵ of the dual CFT is given by $\epsilon \sim e^{-\rho_\infty}$. In this interpretation, the partition function $Z = e^{-I_E}$ with (6.10) looks like that in a $\frac{d}{2}$ dimension CFT. This apparent fractional dimension arises from characteristic profile of the flat EOW brane. As z_0 gets smaller, the region of the flat space where the gravity is present gets expanding, which is give by a d dimensional disk whose the radius is given by $\sqrt{Rz_0}e^{\frac{\rho_\infty}{2}}$. This is consistent with the fact that (6.10) is proportional to $\left(\frac{R}{z_0}\right)^{\frac{d}{2}}$, which may be viewed as a measure of the degrees of freedom.

Our analysis here implies that the gravity dual of d dimensional Euclidean flat Ball B^d with the radius $\sqrt{Rz_0}e^{\frac{\rho_\infty}{2}}$ is given by a certain field theory on another d dimensional ball with the radius $2\sqrt{\frac{R}{z_0}}e^{\frac{\rho_\infty}{2}}$ as follows from (6.1). Indeed if we assume the UV cut off $\epsilon \sim e^{-\rho_\infty}$, its free energy should scale as $e^{\frac{d}{2}\rho_\infty}$, agreeing with (6.10).

7 Conclusions

In this paper, we extensively studied holography with end-of-the-world (EOW) branes whose world volumes are flat, by extending the AdS/BCFT construction [18, 19]. These flat EOW branes have the peculiar feature that they intersect with the boundary of the global AdS on null surfaces. Thus, their gravity duals involve conformal field theories with null boundaries which have not been studied well in the past. Moreover, the brane-world holography relates these to holography for flat spacetimes, which has also been still far from complete understandings.

We classified interesting holographic setups with flat EOW branes into three classes: type I, II and III as in Fig.3. The type I and II setup include a single EOW brane whose tension is negative $T = -\frac{d-1}{R}$ and positive $T = \frac{d-1}{R}$, respectively, in the $d+1$ dimensional bulk. The type III model is defined by the region between two flat EOW branes. The field theory dual of type I is given by a CFT confined inside a diamond with null boundaries. The boundaries look like making the final state projections. On the other hand, in the field theory dual of type II, the CFT on the diamond is coupled to a flat space gravity through its null boundaries. The degrees of freedom of the d dimensional flat space gravity on the brane is dual to those on the null boundaries, whose part can be viewed as the Flat/Carrollian CFT (CCFT) correspondence. In the type III model, the AdS boundary dual to the $d+1$ dimensional bulk is the $d-1$

dimensional null surfaces, which are the boundary of the diamond. Therefore, it singles out the part of the flat/CCFT holography from the type II construction, which can be thought of a version of the wedge holography [39].

By applying the AdS/BCFT description to these setups, we computed holographic entanglement entropy, correlation functions and on-shell actions. We found analytical expressions of holographic entanglement entropy both in type I and type II case, which are simply related to by the transformation $z_0 \rightarrow -z_0$. We noted that in the contributions from the disconnected geodesics in the type II case, there is a constant imaginary part in the entropy, which is similar to the time-like entanglement entropy [45, 46] and we gave a possible explanation in terms of a union of time-like and space-like geodesic. This implies that the dual density matrix is not hermitian. It would be intriguing to consider this from the viewpoint of the recently discussed connection between causal influence and non-hermitian density matrix [65, 66]. Also this phenomenon may not be surprising as the dual of flat space gravity can be non-unitary, which was also pointed out in [52, 67]. We leave more systematic studies of this interesting point for a future work. In both type I and II, there is a phase transition of holographic entanglement entropy between the contributions from the connected and disconnected geodesics by choosing the minimum of the real part of the entropy. We also computed the one-point functions and two-point functions in the type I and II case and found that they are related to each other via the transformation $z_0 \rightarrow -z_0$. These provide strong predictions based on holography for CFTs with null boundaries. In the appendix A, we also performed field theory calculations by taking an infinite boost of a time-like boundary. This leads to a rather trivial result that the one-point function vanishes. It is possible that this corresponds to $z_0 \rightarrow \infty$ limit of type I or type II setup, where the one-point functions also vanish.

In the type III setup, by applying the wedge holography [39], we argued that the $d + 1$ dimensional AdS bulk region between two EOW branes are dual to a $d - 1$ dimensional Carrollian CFT (CCFT), which lives on the null surfaces, which are the edges of a diamond. Since the $d + 1$ dimensional bulk gravity is dual to d dimensional quantum gravity on the two EOW branes, this is essentially reduced to the Flat/CCFT correspondence. In other words, our AdS/BCFT approach gives a justification of the Flat/CCFT correspondence. For example, the analysis of holographic entanglement in this wedge holography reproduces the swing surface prescription of holographic entanglement in flat space holography [48]. Moreover, the analysis of reduction of a scalar

field in the $d + 1$ dimensional bulk to a tower of massive scalar fields in the d dimension brane shows that we can reduce the analysis of holographic correlation functions in the type III case to that in the Flat/CCFT correspondence.

We also studied a Euclidean space version of flat space holography using the flat EOW brane by computing the on-shell action. This implies that the gravity dual of a flat space is given by a point-like theory because the flat EOW brane in the Euclidean AdS intersects with the AdS boundary only at a single point. It would be intriguing to compare this with the celestial holography [11–13] and the Euclidean approach [68] for the better understandings of our new holographic duality.

Acknowledgments

This work is supported by MEXT KAKENHI Grant-in-Aid for Transformative Research Areas (A) through the “Extreme Universe” collaboration: Grant Number 21H05187. TT is also supported by Inamori Research Institute for Science, and by JSPS Grant-in-Aid for Scientific Research (B) No. 25K01000. PH is also supported by the NSFC special fund for theoretical physics No. 12447108. NO is supported by JSPS KAKENHI Grant Number JP24KJ1372. TW is supported by JSPS KAKENHI Grant Number JP25KJ1621.

A BCFT with a null boundary

In this appendix, we analysis the correlation functions in the two dimensional BCFTs with the boundary which is null.

A.1 Free scalar model

We firstly consider the free scalar model,

$$S = \frac{1}{4\pi} \int d\sigma dt (-(\partial_t \phi)^2 + (\partial_\sigma \phi)^2), \quad (\text{A.1})$$

on the cylinder (t, σ) with length L and also the boundary B . The variation gives the equation of motion

$$(-\partial_t^2 + \partial_x^2)\phi = 0, \quad (\text{A.2})$$

and also the boundary condition

$$\text{Dirichlet:} \quad \delta\phi|_B = 0, \quad (\text{A.3})$$

or

$$\text{Neumann:} \quad \nabla_n \phi = 0, \quad (\text{A.4})$$

where n is a unit vector normal to B , and ∇_n is the derivative respect to that direction. The solution in terms of modes is

$$\phi(t, \sigma) = \phi_0 + \frac{4\pi}{L} \pi_0 t + i \sum_{n \neq 0} \frac{1}{n} a_n e^{-\frac{2\pi}{L} i n(t-\sigma)} + i \sum_{m \neq 0} \frac{1}{m} \bar{a}_m e^{-\frac{2\pi}{L} i m(t+\sigma)}. \quad (\text{A.5})$$

We can then impose the Dirichlet boundary condition at the boundary B

$$\sigma = kt, \quad (\text{A.6})$$

which further imposes the constrains on the solution

$$\bar{a}_m = -\frac{1-k}{1+k} a_n, \quad m = \frac{1-k}{1+k} n. \quad (\text{A.7})$$

The green function is calculated from the mode sum

$$\begin{aligned} G_{cyl}(u_1, v_1; u_2, v_2) = & \log \left(1 - e^{-\frac{2i\pi(ku_1+kv_2+u_1-v_2)}{(k+1)L}} \right) + \log \left(1 - e^{-\frac{2i\pi(ku_2+kv_1+u_2-v_1)}{(k+1)L}} \right) \\ & - \log \left(1 - e^{-\frac{2i\pi(k-1)(v_1-v_2)}{(k+1)L}} \right) - \log \left(1 - e^{-\frac{2i\pi(u_1-u_2)}{L}} \right). \end{aligned} \quad (\text{A.8})$$

We can go to the plane limit $L \rightarrow \infty$, and calculate the one-point and two-point functions of the scalar operator $A =: \partial_u \phi \partial_v \phi :$ with $(h, \bar{h}) = (1, 1)$,

$$\langle A(u, v) \rangle = \frac{1-k^2}{((k+1)u + (k-1)v)^2}, \quad (\text{A.9})$$

$$\langle A(u_1, v_1) A(u_2, v_2) \rangle = \frac{(k-1)^2}{\left(\frac{(k-1)v_2}{k+1} + u_1\right)^2 ((k+1)u_2 + (k-1)v_1)^2} + \frac{1}{(u_1 - u_2)^2 (v_1 - v_2)^2}, \quad (\text{A.10})$$

where

$$u = t - x, \quad v = t + x. \quad (\text{A.11})$$

In the case where the boundary is null, we can take $k = \pm 1$ and have

$$\langle A \rangle = 0, \quad \langle AA \rangle = \frac{1}{(u_1 - u_2)^2 (v_1 - v_2)^2}. \quad (\text{A.12})$$

This provides an example of the correlation functions in the BCFTs with null boundary, where the one-point function vanishes and the two-point function is the same as that in the CFT without the boundary. The discussion with the Neumann boundary condition is similar and the direct calculation shows that the one-point and two-point function of A diverges as $\frac{1}{k^2-1}$ and $\frac{1}{(k^2-1)^4}$ as $k \rightarrow \pm 1$. We can normalize A so that it gives the same result as (A.12).

A.2 Analytical continuation and conformal map

We can also consider the one-point function from the analytical continuation and conformal map. In the Euclidean signature, on the plane (x, τ) with the boundary $x = k\tau$, the scalar O with (h, h) has the one-point function

$$\langle O \rangle = \frac{e^{2ih \arctan k}}{(ze^{2i \arctan k} - \bar{z})^{2h}}, \quad (\text{A.13})$$

where we used the transformation

$$z \rightarrow e^{i \arctan k} z, \quad \bar{z} \rightarrow e^{-i \arctan k} \bar{z}, \quad (\text{A.14})$$

from the upper half plane. For the null boundary, we should consider $k \rightarrow \pm i$ so that the boundary is $x = \mp t$ in the Lorentz signature and the one-point function reads

$$\langle O \rangle_{k=\pm i} = 0. \quad (\text{A.15})$$

This also gives the vanishing one-point function in the BCFT if the boundary is null. With the two-point function of two identical scalar with scaling dimension $\Delta = 2h$ on the upper half plane,

$$\langle O_1(z_1, \bar{z}_1) O_2(z_2, \bar{z}_2) \rangle_{UHP} = \left(\frac{\eta}{(z_1 - \bar{z}_1)(z_2 - \bar{z}_2)} \right)^\Delta F(\eta), \quad (\text{A.16})$$

where $\eta = \frac{(z_1 - \bar{z}_1)(z_2 - \bar{z}_2)}{(z_1 - \bar{z}_2)(z_2 - \bar{z}_1)}$ is the cross ratio, we have the two-point function for arbitrary k ,

$$\langle O_1(z_1, \bar{z}_1) O_2(z_2, \bar{z}_2) \rangle_k = \left(\frac{\eta'}{(e^{i \arctan k} z_1 - e^{-i \arctan k} \bar{z}_1)(e^{i \arctan k} z_2 - e^{-i \arctan k} \bar{z}_2)} \right)^\Delta F(\eta'), \quad (\text{A.17})$$

where

$$\eta' = \frac{(e^{i \arctan k} z_1 - e^{-i \arctan k} \bar{z}_1)(e^{i \arctan k} z_2 - e^{-i \arctan k} \bar{z}_2)}{(e^{i \arctan k} z_1 - e^{-i \arctan k} \bar{z}_2)(e^{i \arctan k} z_2 - e^{-i \arctan k} \bar{z}_1)}. \quad (\text{A.18})$$

For the null boundary with $k \rightarrow \pm i$, we find $\eta' \rightarrow 1$ which indicates that the bulk channel is dominant and gives the same two-point function as that in the CFT without boundary,

$$\lim_{k \rightarrow \pm i} \langle O_1(z_1, \bar{z}_1) O_2(z_2, \bar{z}_2) \rangle_k = \langle O_1(z_1, \bar{z}_1) O_2(z_2, \bar{z}_2) \rangle_{\text{CFT}}. \quad (\text{A.19})$$

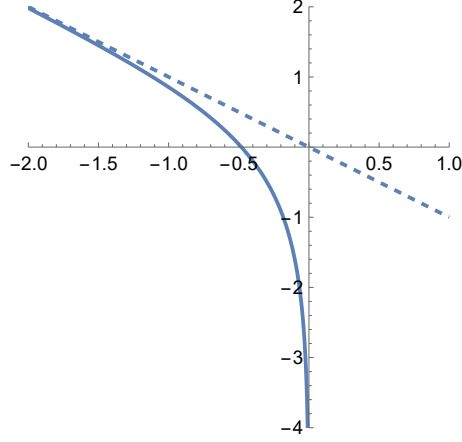


Figure 7. The solid line is the location of the moving mirror, while the dashed line is the null boundary.

A.3 Moving mirror

The null boundary effect can also be considered in the infinitely boosted moving mirror setup as shown in Fig.(A.3) . A static mirror is located at

$$\tilde{x} = 0, \tag{A.20}$$

in the $(\tilde{u} = \tilde{t} - \tilde{x}, \tilde{v} = \tilde{t} + \tilde{x})$ plane. A conformal transformation [69]

$$\tilde{u} = p(u), \quad \tilde{v} = v, \tag{A.21}$$

maps the boundary (A.20) to

$$p(u) = v, \tag{A.22}$$

in the $(u = t - x, v = t + x)$ plane. With a special choice of the map

$$p(u) = -\log(1 + e^{-u}), \tag{A.23}$$

the profile of the boundary is described by

$$t = \log(-2 \sinh x) = \log(e^{-x} - e^x). \tag{A.24}$$

As $t \rightarrow -\infty$, it becomes the usual time-like boundary

$$x = 0. \tag{A.25}$$

As $t \rightarrow \infty$, it becomes null

$$t = -x. \quad (\text{A.26})$$

Then, we can calculate the one-point function of a scalar O with (h, h) in the (u, v) plane from the conformal map, and get

$$\langle O(u, v) \rangle = \frac{p'(u)^h}{(p(u) - v)^{2h}}. \quad (\text{A.27})$$

For fixed v , we can go to the infinitely boosted region from the $u \rightarrow \infty$ limit and have

$$\lim_{u \rightarrow \infty} \langle O(u, v) \rangle = 0. \quad (\text{A.28})$$

Besides, in the (t, x) coordinate,

$$\langle O(t, x) \rangle = \left(\frac{1}{e^{t-x} + 1} \right)^h (-\log(e^{x-t} + 1) - t - x)^{-2h}, \quad (\text{A.29})$$

so that in the limit $t \rightarrow \infty$, we have

$$\lim_{t \rightarrow \infty} \langle O(t, x) \rangle = 0, \quad (\text{A.30})$$

with the null boundary and

$$\lim_{t \rightarrow -\infty} \langle O(t, x) \rangle = \frac{1}{(2x)^{2h}}, \quad (\text{A.31})$$

in the limit $t \rightarrow -\infty$ with the time-like boundary. Then, the similar calculation gives the two-point function with the presence of the mirror,

$$\langle O_1(u_1, v_1) O_2(u_2, v_2) \rangle_{\text{mirror}} = \left(\frac{\eta_p \sqrt{p'(u_1) p'(u_2)}}{(p(u_1) - v_1)(p(u_2) - v_2)} \right)^\Delta F(\eta_p), \quad (\text{A.32})$$

where the cross ratio is

$$\eta_p = \frac{(p(u_1) - v_1)(p(u_2) - v_2)}{(p(u_1) - v_2)(p(u_2) - v_1)}. \quad (\text{A.33})$$

Again, we find that in both $t_{1,2} \rightarrow \infty$ and $u_{1,2} \rightarrow \infty$ limit, $\eta_p \rightarrow 1$ so that the bulk channel is dominant.

References

- [1] G. 't Hooft, *Dimensional reduction in quantum gravity*, *Conf. Proc. C* **930308** (1993) 284 [[gr-qc/9310026](#)].
- [2] L. Susskind, *The World as a hologram*, *J. Math. Phys.* **36** (1995) 6377 [[hep-th/9409089](#)].
- [3] J. M. Maldacena, *The Large N limit of superconformal field theories and supergravity*, *Adv. Theor. Math. Phys.* **2** (1998) 231 [[hep-th/9711200](#)].
- [4] S. S. Gubser, I. R. Klebanov and A. M. Polyakov, *Gauge theory correlators from noncritical string theory*, *Phys. Lett. B* **428** (1998) 105 [[hep-th/9802109](#)].
- [5] E. Witten, *Anti-de Sitter space and holography*, *Adv. Theor. Math. Phys.* **2** (1998) 253 [[hep-th/9802150](#)].
- [6] H. Bondi, M. G. J. van der Burg and A. W. K. Metzner, *Gravitational waves in general relativity. 7. Waves from axisymmetric isolated systems*, *Proc. Roy. Soc. Lond. A* **269** (1962) 21.
- [7] R. K. Sachs, *Gravitational waves in general relativity. 8. Waves in asymptotically flat space-times*, *Proc. Roy. Soc. Lond. A* **270** (1962) 103.
- [8] G. Barnich and C. Troessaert, *Aspects of the BMS/CFT correspondence*, *JHEP* **05** (2010) 062 [[1001.1541](#)].
- [9] A. Bagchi, *Correspondence between Asymptotically Flat Spacetimes and Nonrelativistic Conformal Field Theories*, *Phys. Rev. Lett.* **105** (2010) 171601 [[1006.3354](#)].
- [10] R. Fareghbal and A. Naseh, *Flat-Space Energy-Momentum Tensor from BMS/GCA Correspondence*, *JHEP* **03** (2014) 005 [[1312.2109](#)].
- [11] J. de Boer and S. N. Solodukhin, *A Holographic reduction of Minkowski space-time*, *Nucl. Phys. B* **665** (2003) 545 [[hep-th/0303006](#)].
- [12] S. Pasterski, S.-H. Shao and A. Strominger, *Flat Space Amplitudes and Conformal Symmetry of the Celestial Sphere*, *Phys. Rev. D* **96** (2017) 065026 [[1701.00049](#)].
- [13] S. Pasterski and S.-H. Shao, *Conformal basis for flat space amplitudes*, *Phys. Rev. D* **96** (2017) 065022 [[1705.01027](#)].
- [14] L. Donnay, A. Fiorucci, Y. Herfray and R. Ruzziconi, *Bridging Carrollian and celestial holography*, *Phys. Rev. D* **107** (2023) 126027 [[2212.12553](#)].
- [15] L. Donnay, A. Fiorucci, Y. Herfray and R. Ruzziconi, *Carrollian Perspective on Celestial Holography*, *Phys. Rev. Lett.* **129** (2022) 071602 [[2202.04702](#)].

- [16] A. Bagchi, S. Banerjee, R. Basu and S. Dutta, *Scattering Amplitudes: Celestial and Carrollian*, *Phys. Rev. Lett.* **128** (2022) 241601 [[2202.08438](#)].
- [17] A. Bagchi, P. Dhivakar and S. Dutta, *AdS Witten diagrams to Carrollian correlators*, *JHEP* **04** (2023) 135 [[2303.07388](#)].
- [18] T. Takayanagi, *Holographic Dual of BCFT*, *Phys. Rev. Lett.* **107** (2011) 101602 [[1105.5165](#)].
- [19] M. Fujita, T. Takayanagi and E. Tonni, *Aspects of AdS/BCFT*, *JHEP* **11** (2011) 043 [[1108.5152](#)].
- [20] A. Karch and L. Randall, *Open and closed string interpretation of SUSY CFT's on branes with boundaries*, *JHEP* **06** (2001) 063 [[hep-th/0105132](#)].
- [21] S. Ryu and T. Takayanagi, *Holographic derivation of entanglement entropy from AdS/CFT*, *Phys. Rev. Lett.* **96** (2006) 181602 [[hep-th/0603001](#)].
- [22] S. Ryu and T. Takayanagi, *Aspects of Holographic Entanglement Entropy*, *JHEP* **08** (2006) 045 [[hep-th/0605073](#)].
- [23] V. E. Hubeny, M. Rangamani and T. Takayanagi, *A Covariant holographic entanglement entropy proposal*, *JHEP* **07** (2007) 062 [[0705.0016](#)].
- [24] A. Karch and L. Randall, *Locally localized gravity*, *JHEP* **05** (2001) 008 [[hep-th/0011156](#)].
- [25] S. S. Gubser, *AdS / CFT and gravity*, *Phys. Rev. D* **63** (2001) 084017 [[hep-th/9912001](#)].
- [26] L. Randall and R. Sundrum, *A Large mass hierarchy from a small extra dimension*, *Phys. Rev. Lett.* **83** (1999) 3370 [[hep-ph/9905221](#)].
- [27] L. Randall and R. Sundrum, *An Alternative to compactification*, *Phys. Rev. Lett.* **83** (1999) 4690 [[hep-th/9906064](#)].
- [28] A. Almheiri, R. Mahajan, J. Maldacena and Y. Zhao, *The Page curve of Hawking radiation from semiclassical geometry*, *JHEP* **03** (2020) 149 [[1908.10996](#)].
- [29] A. Almheiri, N. Engelhardt, D. Marolf and H. Maxfield, *The entropy of bulk quantum fields and the entanglement wedge of an evaporating black hole*, *JHEP* **12** (2019) 063 [[1905.08762](#)].
- [30] G. Penington, *Entanglement Wedge Reconstruction and the Information Paradox*, *JHEP* **09** (2020) 002 [[1905.08255](#)].

- [31] K. Suzuki and T. Takayanagi, *BCFT and Islands in two dimensions*, *JHEP* **06** (2022) 095 [[2202.08462](#)].
- [32] K. Izumi, T. Shiromizu, K. Suzuki, T. Takayanagi and N. Tanahashi, *Brane dynamics of holographic BCFTs*, *JHEP* **10** (2022) 050 [[2205.15500](#)].
- [33] S. Cooper, M. Rozali, B. Swingle, M. Van Raamsdonk, C. Waddell and D. Wakeham, *Black hole microstate cosmology*, *JHEP* **07** (2019) 065 [[1810.10601](#)].
- [34] S. Antonini and B. Swingle, *Cosmology at the end of the world*, *Nature Phys.* **16** (2020) 881 [[1907.06667](#)].
- [35] M. Van Raamsdonk, *Cosmology from confinement?*, *JHEP* **03** (2022) 039 [[2102.05057](#)].
- [36] H. Omiya and Z. Wei, *Causal structures and nonlocality in double holography*, *JHEP* **07** (2022) 128 [[2107.01219](#)].
- [37] S. Antonini, P. Simidzija, B. Swingle and M. Van Raamsdonk, *Cosmology from the vacuum*, *Class. Quant. Grav.* **41** (2024) 045008 [[2203.11220](#)].
- [38] C. Waddell, *Bottom-up holographic models for cosmology*, *JHEP* **09** (2022) 176 [[2203.03096](#)].
- [39] I. Akal, Y. Kusuki, T. Takayanagi and Z. Wei, *Codimension two holography for wedges*, *Phys. Rev. D* **102** (2020) 126007 [[2007.06800](#)].
- [40] Y. Chen, V. Gorbenko and J. Maldacena, *Bra-ket wormholes in gravitationally prepared states*, *JHEP* **02** (2021) 009 [[2007.16091](#)].
- [41] P.-X. Hao, T. Kawamoto, S.-M. Ruan and T. Takayanagi, *Non-extremal Island in de Sitter Gravity*, [2407.21617](#).
- [42] Z. Wei, *Holographic Dual of Crosscap Conformal Field Theory*, [2405.03755](#).
- [43] K. Fujiki, H. Kanda, M. Kohara and T. Takayanagi, *Brane cosmology from AdS/BCFT*, *JHEP* **03** (2025) 135 [[2501.05036](#)].
- [44] Y. Nakata, T. Takayanagi, Y. Taki, K. Tamaoka and Z. Wei, *New holographic generalization of entanglement entropy*, *Phys. Rev. D* **103** (2021) 026005 [[2005.13801](#)].
- [45] K. Doi, J. Harper, A. Mollabashi, T. Takayanagi and Y. Taki, *Pseudoentropy in dS/CFT and Timelike Entanglement Entropy*, *Phys. Rev. Lett.* **130** (2023) 031601 [[2210.09457](#)].
- [46] K. Doi, J. Harper, A. Mollabashi, T. Takayanagi and Y. Taki, *Timelike entanglement entropy*, [2302.11695](#).

- [47] M. P. Heller, F. Ori and A. Serantes, *Geometric Interpretation of Timelike Entanglement Entropy*, *Phys. Rev. Lett.* **134** (2025) 131601 [[2408.15752](#)].
- [48] L. Apolo, H. Jiang, W. Song and Y. Zhong, *Swing surfaces and holographic entanglement beyond AdS/CFT*, *JHEP* **12** (2020) 064 [[2006.10740](#)].
- [49] D. Neuenfeld, *The Flat-Space Limit of AdS Coupled to a Bath*, [2508.03798](#).
- [50] H. Kanda, T. Kawamoto, Y.-k. Suzuki, T. Takayanagi, K. Tasuki and Z. Wei, *Entanglement phase transition in holographic pseudo entropy*, *JHEP* **03** (2024) 060 [[2311.13201](#)].
- [51] H. Kanda, M. Sato, Y.-k. Suzuki, T. Takayanagi and Z. Wei, *AdS/BCFT with brane-localized scalar field*, *JHEP* **03** (2023) 105 [[2302.03895](#)].
- [52] N. Ogawa, T. Takayanagi, T. Tsuda and T. Waki, *Wedge holography in flat space and celestial holography*, *Phys. Rev. D* **107** (2023) 026001 [[2207.06735](#)].
- [53] C. Nunez and D. Roychowdhury, *Interpolating between Space-like and Time-like Entanglement via Holography*, [2507.17805](#).
- [54] M. P. Heller, F. Ori and A. Serantes, *Temporal Entanglement from Holographic Entanglement Entropy*, [2507.17847](#).
- [55] H. Jiang, W. Song and Q. Wen, *Entanglement Entropy in Flat Holography*, *JHEP* **07** (2017) 142 [[1706.07552](#)].
- [56] A. Bagchi, R. Basu, D. Grumiller and M. Riegler, *Entanglement entropy in Galilean conformal field theories and flat holography*, *Phys. Rev. Lett.* **114** (2015) 111602 [[1410.4089](#)].
- [57] C. A. Bayona and N. R. F. Braga, *Anti-de Sitter boundary in Poincare coordinates*, *Gen. Rel. Grav.* **39** (2007) 1367 [[hep-th/0512182](#)].
- [58] J. Kastikainen and S. Shashi, *Structure of holographic BCFT correlators from geodesics*, *Phys. Rev. D* **105** (2022) 046007 [[2109.00079](#)].
- [59] D. Z. Freedman, S. D. Mathur, A. Matusis and L. Rastelli, *Correlation functions in the CFT(d) / AdS(d+1) correspondence*, *Nucl. Phys. B* **546** (1999) 96 [[hep-th/9804058](#)].
- [60] M. Ammon and J. Erdmenger, *Gauge/gravity duality: Foundations and applications*. Cambridge University Press, Cambridge, 4, 2015, [10.1017/CBO9780511846373](#).
- [61] V. Balasubramanian and S. F. Ross, *Holographic particle detection*, *Phys. Rev. D* **61** (2000) 044007 [[hep-th/9906226](#)].

- [62] E. Hijano and C. Rabideau, *Holographic entanglement and Poincaré blocks in three-dimensional flat space*, *JHEP* **05** (2018) 068 [[1712.07131](#)].
- [63] E. Hijano, *Flat space physics from AdS/CFT*, *JHEP* **07** (2019) 132 [[1905.02729](#)].
- [64] K. Nguyen, *Carrollian conformal correlators and massless scattering amplitudes*, *JHEP* **01** (2024) 076 [[2311.09869](#)].
- [65] T. Kawamoto, R. Maeda, N. Nakamura and T. Takayanagi, *Traversable AdS wormhole via non-local double trace or Janus deformation*, *JHEP* **04** (2025) 086 [[2502.03531](#)].
- [66] A. Milekhin, Z. Adamska and J. Preskill, *Observable and computable entanglement in time*, [2502.12240](#).
- [67] S. Pasterski and H. Verlinde, *Chaos in celestial CFT*, *JHEP* **08** (2022) 106 [[2201.01630](#)].
- [68] W. Li and T. Takayanagi, *Holography and Entanglement in Flat Spacetime*, *Phys. Rev. Lett.* **106** (2011) 141301 [[1010.3700](#)].
- [69] I. Akal, T. Kawamoto, S.-M. Ruan, T. Takayanagi and Z. Wei, *Zoo of holographic moving mirrors*, *JHEP* **08** (2022) 296 [[2205.02663](#)].